Politecnico di Torino

Politecnico di Torino

Master's Degree in Nanotechnologies for ICTs

Bismuth oxynitrates nanostructures for electrochemical sensors modification:

Paracetamol, Dopamine and Uric Acid sensing

Master's Thesis Project

Gianluigi Rodia

302313

Supervisors:

Prof. Alberto Tagliaferro (PoliTo)

Prof. Sandro Carrara (EPFL)

Dr. Mattia Bartoli (PoliTo)

A.Y. 2022/2023 – October 2023

If you thought before that science was certain -well,

that is just an error on your part.

-Richard Feynman

Acknowledgements

At the conclusion of this thesis project, I would like to express my sincerest thanks to the people I have worked with over the past months.

First, I would like to thank Prof. Alberto Tagliaferro and Prof. Sandro Carrara for giving me the opportunity to participate in this interesting project and to get in touch with their work. My sincere thanks to all the people I met and worked with in the laboratories of the Carbon Group at the Politecnico di Torino and the BCI at EPFL. I enjoyed working with you and getting to know all your stories. Particularly important is my thanks to Dr. Mattia Bartoli for making me understand what it means to work with passion and how not to stop at the superficialities of a result.

Finally, I would like to thank all the friends that I met over these years and my parents for their constant support.

Abstract

Nowadays, the use of sensors has achieved great importance in various fields. Agriculture, pollution detection, and food safety are just some of the fields that have demanded the use of increasingly precise and accurate sensors. Of all of them, the medical field has paid great attention to the use of sensors in diagnosing and treating diseases. The use of drugs for surgical or therapeutic purposes involves careful attention to the doses administered to the patient. Overdosing a specific drug can lead to organ transplantation and/or malfunctioning of apparatuses and systems. An example is the use of paracetamol as a pain-relieving and antipyretic agent, the improper use of which can lead to liver and kidney failure. The onset of disease is often associated with changes in particular chemicals in the body, as is the case with dopamine levels in the brain that can be an alarm bell for Parkinson's disease or uric acid levels associated with gout. This is why the importance of accurate and stable detection of quantities of chemical species arises. Electrochemical sensors have great potential by acting as sensitive and inexpensive devices.

The world of nanomaterials represents a great possibility for achieving this goal. In recent years, various nanostructures have been used to improve the performance of electrochemical sensors. In the list of materials, bismuth has a great reputation due to the high stability of its nanostructures and its biocompatibility. In this project, several bismuth nitrates were synthesised and used to modify electrodes (DropSens 100) to detect paracetamol, dopamine, and uric acid in a neutral solution. Particular attention was given to the synthesis process in which different amounts of PEG were used. The latter takes on the role of a surfactant in the production of the materials, which can lead to greater stability of the dispersed phases and particular morphological characteristics of the final product.

Once the materials were synthesised, they were analysed using analysis techniques such as Raman and IR spectroscopy and the use of SEM.

The modified sensors were compared to the bare sensor using the cyclic voltammetry technique. The interaction between electrodes and analyte was studied for different scan rates to derive kinetic constant rate and transfer coefficients. The latter two, derived using Laviron's theory, were used to compare the electrochemical properties of the sensors. The analyses showed that the use of high concentrations of PEG (2 to 4 times the amount of bismuth salts) in the synthesis process is linked to an increase in the constant rate. For the paracetamol detection, it was obtained a value of 5.72 ± 0.67 ms^{-1} and for the dopamine detection a value of 42.82 ± 0.48 ms^{-1}.

The performances of the various sensors were also evaluated by changing the analyte concentrations to reconstruct the calibration curves.

Bismuth nanostructures made it possible to realise more sensitive sensors by increasing the sensitivity. The electrode modified with bismuth oxynitrates produced with 4 times the amount of PEG with respect to the bismuth salts weight presented a sensitivity of 42.82 ± 0.48 $\mu A/mM$ for the paracetamol detection, 16.67 ± 1.31 $\mu A/mM$ for the dopamine detection and 9.59 ± 0.41 $\mu A/mM$ for the uric acid.

The electrochemical analyses carried out in this work were aimed at highlighting the electrocatalytic properties of bismuth and the role that a surfactant such as PEG plays in the synthesis of materials.

Contents

List of Figures

List of Tables

1 Introduction

Sensors and biosensors have been the subject of much attention from the middle of the last century to the present. Nowadays, the development of new sensors is one of the main research fields in science and it will be in the future. Sensing devices draw attention from several science fields, such as material science, chemistry, electrochemistry, physics and engineering which lead to different degrees of freedom in the development and improvement of new sensors and new techniques.

Nanotechnology is related to the synthesis and use of new processes, devices, and materials at the atomic or molecular scale. It is completely one of the most studied fields, considering its recent evolution. This represents a powerful tool that could be employed to improve the sensitivity and the efficiency of sensing technique.

1.1 Sensors and Biosensors

Sensors play a crucial role in collecting data that allows us to understand and control the specific entity under study. A sensor detects changes in a particular system and converts it into a signal. It belongs to a wider device category that relates a particular input to a different type of output. These types of devices are:

- Transductor: a device that converts energy and takes advantage of its production
- Actuator: a device that has movable components
- Sensor: a device that responds to an external stimulus
- Detector: a device that extrapolates a signal

A sub-category of a sensor is one related to the “BIO” world. They are called Biosensors and they are designed to detect and measure biological substances and processes. The working principle of a sensor is formed by two different components: the receptor and the transducer.

The receptor (called probe in case of DNA analysis) is responsible for the analyte recognition. For this reason, it is the part of the device that is in direct contact with the sample, and it directly identifies the analyte or immobilises it through particularly selective sites. The transducer has a physical role of the device, it converts the presence or the modification of the element in a signal.

Important is the match and the integration between the receptor and the transducer because the lesser the interference allowed by the coupling, the better the sensitivity of the sensor.

As shown in Figure 1 a sensor is usually linked to a backend part that includes also all the electronic part that allows a simple read of the signal [1].

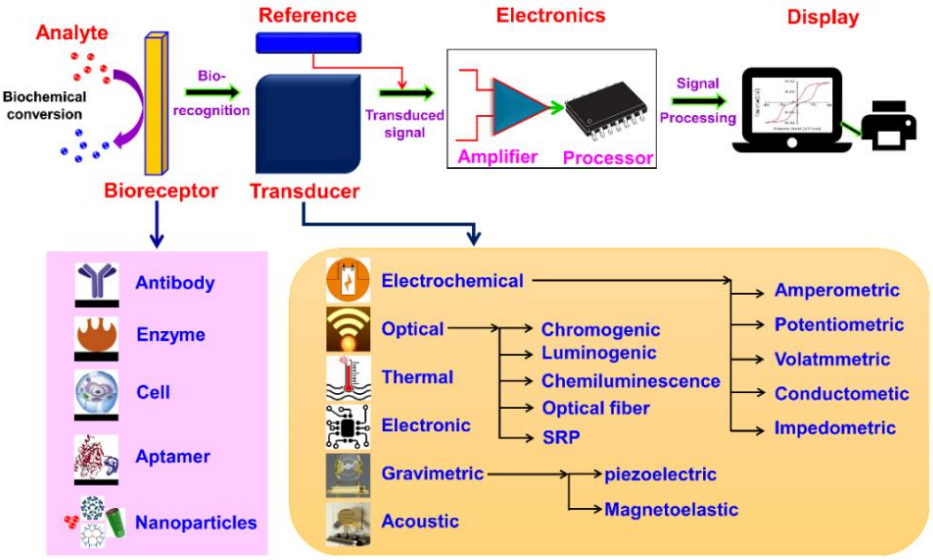

Figure 1 – Schematics of the principal components of a biosensors and list of the different types of transducers [1]

In the case of biosensors, the element under analysis could be enzymes, antibodies, or living cells. After the conversion, the transducer could generate an electrical, optical, mechanical, or even a measurable signal. The goal is to obtain a signal proportional to the concentration of the analyte under study. This type of signal is the base for the categorization of the different electronic configurations of a biosensor:

- Electrochemical signal: Amperometric electrodes

  It is a system that generates an electric signal based on the oxidation or reduction of an electroactive species on an electrode surface. The measured current is proportional to the concentration of the analyte. It is a powerful system for clinical use considering that it can detect concentrations up to the nanomolar or the micromolar range [2].

- Heat signal: thermocouples and thermistors

  Usually, they are known as thermal biosensors, and they measure the enthalpy of the reaction that occurs on the surface of the device. An example is the thermometric enzyme-linked immunosorbent assay (TELISA), a modification of the classic ELISA process that involves the detection of biomolecules through colour changes or fluorescence. In TELISA the enzyme heat formation is measured using an enzyme thermistor and it showed great results in the determination of the human serum albumin in the nanomolar range [3].

- Mechanical signal: micrograviметric detectors

The use of a microscopic cantilever, usually made of Silicon or other types of metals, could give a fast response time and an efficient system immune to any external noise. The approach of the target on the surface of the cantilever generates a deflection of the structure or a change in resonance frequencies due to a mechanical measurable stress. It is a method widely used especially in the medical field and in research showing the possibility to be integrated with other systems to improve its performance [4].

- Voltage drops: Field-effect transistors (FET)

FETs are electronic devices widely used in integrated circuits. They present a sort of electronic channel in which electrons can flow. The voltage control on the terminal (Gate) could allow or modulate the electron (or holes) passage. This device could be used in sensing and exploiting the Gate as an active part. In this sense, the device became ion-sensitive and took the name of ISFET (ion sensitive-FET). If the analyte comes in contact with the Gate, a voltage drop occurs that could be proportional to the type and/or to the concentration of the analyte. The ENFET (enzymatic-FET) is a particular type of device that presents an enzyme on top of the active part responsible for the reception of the target [5].

- Light signal: optoelectronic device

This device exploits the change of light intensity emitted by a dye immobilized on the active surface, which is usually an optical fiber. This system is associated with a light-emitting diode to detect the emission of light by the dye. Another interesting mechanism is the exploiting of an evanescent wave component of a light beam which allows the capability of real-time measurement avoiding any electrochemical interference [6].

In this large panorama, every type of sensor takes advantage of the case in which it is enrolled, as no single sensor type is ideal for all situations. Amperometric sensors take advantage of several characteristics: selectivity to a particular analyte, high sensitivity, mid/long-term stability, miniaturization, fast response time and low operating cost [7].

Another difference in the category of electrochemical sensors is the mechanism of approaching the analyte. This process could be direct between the target and the active site or indirect, using a “helper” that has the role of biorecognition. This help could be chosen by a wide category of enzymes that are placed on the top of the active site. An enzyme is a highly selective protein able to catalyse metabolic reactions and this type of device is called enzymatic sensors. The main advantage of this type of device is the high specificity because enzymes typically have a specific affinity for the substrates, ensuring the reaction only with their target. The efficiency of the enzymatic sensors

relies completely on their enzyme, making them not suitable for extreme and external conditions. Temperature, humidity, pH and light could modify the efficiency of the sensor interacting with the enzymes.

Nonenzymatic sensors are often more robust. The versatility of this type of sensor allows the use of them in a broader range of conditions, making them suitable for several applications. Nonenzymatic sensors employ non-biological elements to respond and detect the target, such as metals, metal oxides and polymers. The interaction with the analyte is based on chemical and physical interactions, which include processes like covalent binding or adsorption.

All the electrochemical sensors are employed in a multitude of applications, ensuring an efficient detection option for expensive and complex analytical instruments. Pollutants detection and control systems are two of the fields of application of electrochemical sensors considering the necessity of fast and sensitive analysis. These devices have proven to be effective in the detection of benzene[8], nitrite[9], or heavy metals such as Mercury (Hg) [10] and Lead (Pb) [11].

Many solutions have been proposed also in the field of food safety in the detection of allergens, antibiotics, toxins, bacteria, and viruses. These solutions have improved drastically the process of production especially at the beginning of its cycle reducing cost of the production and avoiding food waste.

Probably the main application in which electrochemical biosensors have found the main success is the clinical and therapeutic field. Nowadays it is crucial the role of the prevention of disease and early diagnosis. A lot of research has been done on numerous types of analytes and it has still a great potential for future applications. Suitable options have been found in the detection of glucose, lactate, cholesterol, antigens, antibodies, DNA and cancer markers [12].

A complete revolution of the electrochemical detection branch was the integration with MEMS technology. MEMS is the acronym for microelectronic-mechanical systems, and it refers to all the miniaturized devices used to create integrated and smart systems. They integrate multiple functions in a single device, increase the performance and reduce the cost and the time of processes through the miniaturization of the structure. With the integration of MEMS in biomedical and biochemical applications, the research has opened the road to the BIOMEMS world [13]. They are called also Lab On a Chip (LOC) to highlight the powerful advantage of miniaturization that allows to provide the functions of a laboratory on a micrometric scale.

LOC paved the way for a new degree of freedom in the development of biosensors. It is given by the choice of the material employed in the fabrication such as PMMA, Polystyrene, Polycarbonate, and Oxides. Several fabrication techniques could be employed, like micromachining, laser ablation, hot embossing and injection moulding [14].

1.2 Paracetamol

Paracetamol (PCM), called also Acetaminophen is a widely used medication for different purposes. Its use is related to its analgesic, anti-inflammatory and antipyretic effects on the body. This drug is usually used to relieve pain and reduce fever. One of the most common and delicate uses is the paracetamol injection in the body during a medical operation through a constant injection to control the analgesic effect on the body. Sometimes the problem of the amount of paracetamol in the body could be a problem due to its overdosage toxic effect. One of the main problems, caused by an excessive dosage is the induction of iatrogenic hypotension, in particular in the case of intravenous administration [15].

Nowadays a lot of studies are focused on the understanding of the mechanisms of toxicity on the body and the differences between the different administrations.

The liver metabolized the paracetamol through the action of several enzymes, like cytochrome P450 (CYP) enzymes. These enzymes oxidase the paracetamol molecules generating N-acetyl-p-benzoquinone (NAPQI) that represent the main metabolites of the paracetamol. Normally NAPQI is detoxified by reaction with glutathione produced by the liver, but the presence of a high level of NAPQI can be toxic and it can accumulate and cause liver damage.

A metabolite accumulation of paracetamol could cause damage to the liver during the body assimilation [16] and to the kidney for the expulsion of the excess PCM [17].

Due to the problem of checking the exact paracetamol presence in real-time and in an accurate way different techniques were developed. Such important techniques are chemiluminescence[18], spectrofluorimetry [19] and spectrophotometry[20].

An effective idea to check the presence and quantify the amount was represented using its electroactive properties. The ability to oxidase rapidly the paracetamol molecule allowed the spreading of the electrochemical technique use. This method represents one of the most suitable due to its rapidity and high sensitivity. Also, the use of electrodes allows to increase in the number of degrees of freedom through the study of the well-suited electrode material for PCM detection.

Different structures were been under study with particular attention to the geometry and the type of nanostructure[21]. These nanostructures were built or immobilized on the working electrode to exploit their catalytic effect. Some of them include the use of silver NPs [22], polymer NPs [23], and γ-Fe2O3/CNTs [24].

1.3 Dopamine

Dopamine (DA) is the most famous among the catecholamines and it is one of the most important neurotransmitters. It plays an important role in the function of the central nervous system, but it is also related to some important functions of the cardiovascular system, the hormonal and the renal ones [25]. The DA is bio-synthesized starting from the amino acid tyrosine by the central nervous system and then stored in synaptic vesicles. A specific synaptic impulse could be sent to the vesicles to allow the release of dopamine for its function. Its main role is related to the modulation of synaptic impulses in different brain sections, such as impulses related to behaviour, learning, memory, dreaming, needs and regulation of prolactin production [26].

The role of dopamine is crucial also in the recognition of several neuronal diseases. Parkinson's disease is a well-known pathology related to a progressive loss of coordination in movement [27]. It is a neurodegenerative disorder that affects the nervous system over time causing damage in parts of the brain. Parkinson's and Alzheimer's diseases are the most common disorders that involve the clinical condition of 2-3% of the population over 60 years. This condition is due to the progressive degeneration of dopaminergic neurons in the substantia nigra pars compacta, a mesencephalic site where dopamine is produced [28]. The treatment of this disease provides the use of dopaminergic antiparkinsonian agents that have the aim of mimicking the dopamine action in the nervous system. Some patients have shown good responses to the treatment when the diagnosis is done at the early stages of the disease. If Parkinson is diagnosed too late the effect of the dopaminergic agents does not result effectively since a good part of the nervous system is damaged [29]. In this panorama, it is important to have the diagnosis of the disorder at the right time of the evolution. Due to the correlation between the level of dopamine in the brain and the progress of the disease, the detection of dopamine present in a specific site becomes important in the treatment.

The detection of dopamine is a process that has involved conventional methods such as ELISA [30], HPLC [31], and spectrophotometry [32]. These techniques are generally expensive, time-consuming, and impossible to use on-site. During a surgical intervention, it is necessary to have a fast and sensitive detection of the interested analyte. A solution comes from the characteristic of dopamine to be an electroactive molecule. Electrochemical sensors represent a suitable option for the determination of dopamine in a more direct way. Several studies have reported the performances of several electrochemical sensors based on metal oxide NPs, graphene, polymers, carbon nanotubes, and ionic liquids [33].

The nature of the modifier has shown direct effects on the performances of the sensor in terms of sensitivity and stability, and this has opened the electrochemical sensing field

to the research of different structures and materials with respect to the application of the sensor.

1.4 Uric Acid

Uric Acid (UA) is a product of the breakdown of purines that are present in the food or the body. It flows in the blood freely or is linked to transport proteins [34]. Kidneys are the organs responsible for the depuration of the blood and then for the expulsion of the uric acid. In specific physiological roles, it acts as an antioxidant defining its important presence in the body.

Excessively high levels of uric acid could be dangerous for human health. The condition is known as hyperuricemia and it is linked to a great production of the molecule or a low level of excretion. The most notable complication is gout, a sort of inflammatory arthritis that affects joints and in less-impact tissues [35]. The gout is due to the formation of needle-shaped monosodium urate crystals that accumulate in joints. The treatment of this disease is characterized by the use of anti-inflammatory drugs (NSAIDs) combined with the use of drugs that lower the level of uric acid in the body [36]. Also, low concentration of uric acid in the blood could be a symptom of genetic disease. This represents the need for a fast and accurate detection method able to measure the level of uric acid in urine samples, human serum, saliva, and other biological fluids.

Some solutions for uric acid detection are given by spectral techniques (UV and fluorescence), chromatography, and capillary electrophoresis [37]. These techniques have good stability and quite accurate sensitivity, but they have a high cost and they are complex in terms of process and sample preparation.

The electrochemical detection method represents a well-known solution due to its affordability, fast response, and simple operation. In the list of enzymatic biosensors used in the detection of uric acid, the most important is the one based on urate oxidase (UO). The use of this enzyme allows the reaction with the uric acid and the dissolution of oxygen that is directly proportional to the UA concentration [38].

Also, the use of non-enzymatic biosensors has acquired a lot of attention in the detection of uric acid due to their good sensitivity and stability. Different nanostructures have been widely employed due to their electrocatalytic effects, such as multi-wall carbon nanotubes [39], one-dimensional MgO [40] and ZnO nanorods [41].

1.5 Bismuth

The development of non-enzymatic electrochemical biosensors could involve the employment of bare electrodes or modified ones using nanostructures. The latter represents a new degree of research concerning the materials and the shape of the structure involved. In the list of materials of the periodic table, particular attention is given to Bismuth due to its unique physical and chemical properties. It is a semi-metal and the most stable with a high atomic number (Z = 83) on the Earth.

Its crystalline structure is very similar to the arsenic and antimony ones. At normal conditions, it crystallizes in a rhombohedral lattice, but under an external stimulus like pressure and temperature could assume several polymorphisms, such as monoclinic B-II, tetragonal B-III, or bcc Bi-V [42]. Bismuth compounds are used in different forms with specific synthesis methods. Bismuth halides are prepared from the bismuth oxides in a water-based medium by adding the relative acid. Bismuth oxide halides are synthesized by partial hydrolysis of bismuth halides or through a thermal process. Bismuth oxides and bismuth nitrates could be prepared by solid state-method by thermal decomposition [43].

Bismuth nanoparticles have been used in several applications due to their high surface area-to-volume ratio, and dimension-tuneable optical and electronic properties. Despite its high atomic number, it is known as a 'green element' due to its safety and biocompatibility which allows its use in the medical field. Bismuth NPs are employed as contrast agents in medical imaging, and antibacterial activity against a wide range of microorganisms. Several publications document the activity of bismuth NPs against the growth of including Staphylococcus aureus [44] and Pseudomonas aeruginosa [45].

In the pharmaceutic field, the bismuth is employed in the production of specific drugs. To treat a set of gastrointestinal disorders, bismuth subsalicylate ($C_7H_5BiO_4$) is a well-known compound for the production of Pepto-Bismol [46].

Bismuth nanoparticles or bismuth nanostructures with other materials are used also as catalysts in chemical reactions, especially in green science. Some examples in material science showed that Bismuth-coated iron NPs can accelerate the reductive degradation of chloramphenicol with applications in green energy production [47], or that Bismuth structures could be used as catalysts for the reduction of CO_2 [48].

1.6 Electrochemistry and Electrochemical Sensor

In the previous section, the general panorama of sensors is presented, and particular attention is reserved on the potential of electrochemical sensors. Electrochemistry is the

branch that examines the effect of the chemistry process that leads to electrical effects. The main phenomenon is the electron transfer between species that is exploited in the oxidation/reduction of them. These processes could be explained from several points of view, but they always present the same denominator: the transport of an electron by a Donor specie to an Acceptor specie.

$$D + A \rightarrow D^{+} + A^{-} \tag{1.1}$$

The oxidation/reduction of a specific specie is the modification of the number of electrons in the atom Outer Shell. This is related to a change in the oxidation state (or oxidation number), a sort of "formal" charge that characterizes the atom about the electron distribution with the other atom which creates a bond. An increase of the oxidation number is associated with the acquisition of positive charge, it means that the atom has lost electrons and it is said it is oxidated. The reduction is the inverse process. It is associated with a decrease in the oxidation number, the atom has acquired electrons.

During the mid-20th century, a variety of theoretical studies have been done in the electron transfer field. Libby [49] and Randles [50] discussed the process through the influence of the Frank-Condon principle [51] and they introduced the concept of the potential energy curve. R.J. Marcus, Zwolinki and Eyring [52] and Weiss [53] consider a more quantum point of view. They introduced in the discussion the concept of electron tunnelling in terms of barrier height and transfer probabilities. A few years later, Hush [54] adopted charge density parameters to treat differently the calculation of the electron transfer and introduced also the thermodynamic nature of the process.

The most famous and large work on the electron transfer process is attributed to R.A. Marcus [55], who received the Nobel Prize in chemistry in 1992. His theory explains the mechanism behind the rate of electron transfer using the dielectric polarization vector to characterize the solvent behaviour and the reaction Gibbs free energy ΔG^{o}.

All the theories previously listed present some common bases. First, they consider the description under the two-state approximation, where the process is described by two states: the initial one, where the Reagents of the process exist and are ready to interact to let the transfer happen. The final state is represented by the Products of the reaction. The description of the state is based also on the Adiabatic or Born-Oppenheimer approximation, for which the nucleus of the atom is considered fixed with respect to the motion of the electron in the external shells. This approximation is commonly used in quantum chemistry and solid-state physics since allows to simplifies the Schrodinger equation in the Hamiltonian description of the molecular system. This approximation is often accepted because the nucleus of an atom is heavier with respect to the electron mass, this led to a fast modification of the electronic system with respect to the nuclear one. Then from the quantum point of view, it is possible to describe the two states with two eigenstates: φ_i for the initial state and φ_f the final state.

Considering a general expression like (1.1) where a general electron transfer is presented, we should distinguish how the molecules are coupled. We consider diabatic states if the molecules are uncoupled and the system is described by

$$H^0\varphi_i = \varepsilon_i \varphi_i \tag{1.2a}$$

$$H^0\varphi_f = \varepsilon_f \varphi_f \tag{1.2b}$$

where H^0 is the equilibrium electronic Hamiltonian that describes the evolution of the system, ε_i and ε_f are the eigenenergies associated to the states. In this situation, the two states are considered as non-interacting and the electron transfer probability is null. On the contrary, if the two systems are coupled, we are considering adiabatic states, which means that there is an electron coupling J, called sometimes transfer integral. In this case, the matrix description is

$$\begin{pmatrix} H^0 & J \\ J & H^0 \end{pmatrix}\begin{pmatrix} \varphi_+ \\ \varphi_- \end{pmatrix} = \begin{pmatrix} \varepsilon_+ & 0 \\ 0 & \varepsilon_- \end{pmatrix}\begin{pmatrix} \varphi_+ \\ \varphi_- \end{pmatrix} \tag{1.3}$$

With φ_+ and φ_- eigenfunctions of coupled states.

The electronic coupling energy J is defined as

$$J = \langle \varphi_i | H^0 | \varphi_f \rangle \tag{1.4}$$

The energy of the coupled states is given by the combination of the initial and final one ε_i and ε_f :

$$\varepsilon_+ = \frac{\varepsilon_i + \varepsilon_f}{2} + \sqrt{\frac{(\varepsilon_i + \varepsilon_f)^2}{2} + J^2} \tag{1.5a}$$

$$\varepsilon_- = \frac{\varepsilon_i + \varepsilon_f}{2} - \sqrt{\frac{(\varepsilon_i + \varepsilon_f)^2}{2} + J^2} \tag{1.5b}$$

The graphical description of the system is given through the representation of the potential energy profile in Figure 2, where the potential profiles of adiabatic and non-adiabatic systems are shown. They are presented as a function of nuclear reaction coordinate Q. The variable Q is a general expression of the spatial coordinate of the state and includes bond lengths, bond angles, and rotations. If for example the system is formed by a diatomic molecule, the coordinate Q represents only the distance between the atoms.

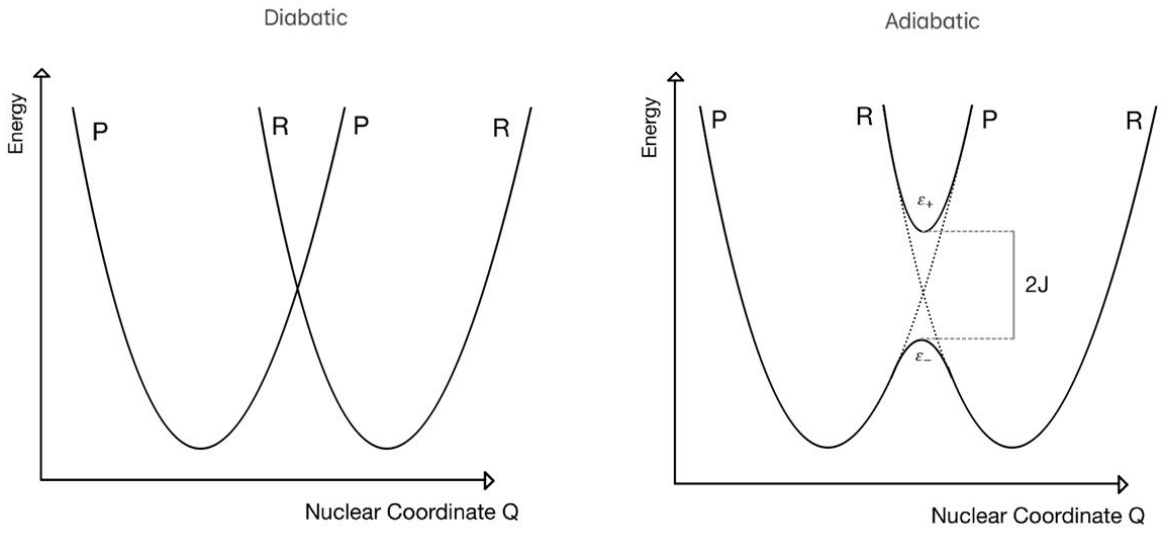

Figure 2 – Potential energy profiles of adiabatic and non-adiabatic systems

From Figure 2 it is deduced that in a diabatic process, the interaction between the initial and the final state is null, or it is so small that the electronic coupling J is considered close to zero. This is the case in which reactants and products surfaces no longer interact considerably.

In adiabatic processes, J is moderately large, leading to the interaction of the Potential surface energies. The surfaces are separated in the intersection region and the distance between them is equal to 2J.

If the system is represented in terms of Gibbs free energy, it is remarked that the profile dependence of the nuclear coordinate is represented as a parabola [56]. Then in the discussion, it is possible to use both profiles. From the transition state theory (TST) the first order rate constant k is determined on the activation energy of the process ΔG^{+}, in an Arrhenius-like dependence:

$$k = k_{el} \upsilon_n exp\left[\frac{-\Delta G^{+}}{k_B T}\right] \quad (1.6)$$

In the previous formula k_{el} is the electronic transmission coefficient (equal to 1 in the classic point of view), υ_n is the frequency of passage through the transition state, k_B is the Boltzmann constant and T is the temperature [57].

An important parameter in the discussion is the reorganization energy λ defined as the energy variations if the reagents were to assume the configuration of the products without any transfer of electrons. Other important terms are the Gibbs energy of activation for the electron transfer ΔG^{*} and the difference in energy of the equilibrium states between the products and the reagents ΔG^{0}. Graphically they are presented in Figure 3:

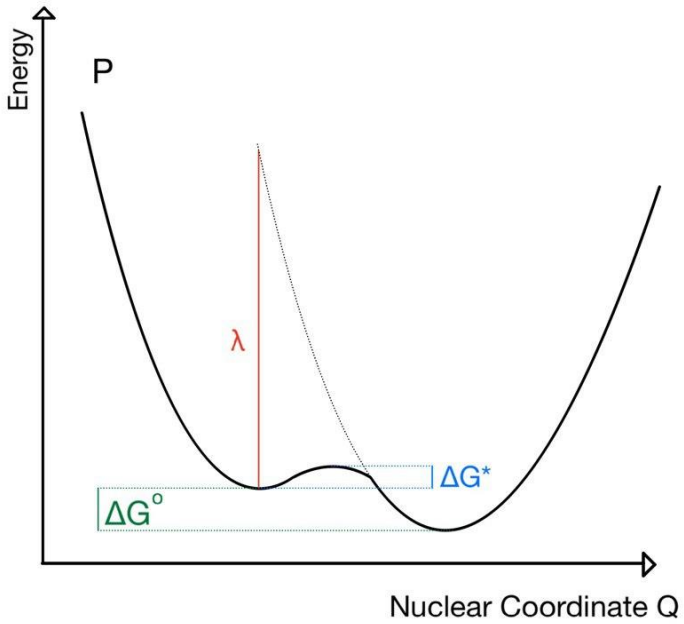

Figure 3 – General configuration of a diabatic system

After several calculations it is possible to express ΔG^* in terms of reorganization energy:

$$\Delta G^* = \frac{(\lambda+\Delta G^0)^2}{4\lambda} \tag{1.7}$$

Combining the two previous formulas (1.6 and 1.7) it is possible to obtain the classical Marcus equation

$$k = k_{el} \upsilon_n exp\left[-\frac{(\lambda+\Delta G^0)^2}{4\lambda\, k_B T}\right] \tag{1.8}$$

In the final formulation expressed in (1.8) it is represented the dependence of the electron transfer rate k with the Gibbs free energy of reaction ΔG^0, underlying the importance of the initial and final configuration of the system.

The theory postulated by Marcus is based on two important classical assumptions that simply the problem under study [58]:

- Dielectric continuum model

  This model considers the solvent in which the process takes place as a dielectric continuum. On this approximation, we define the reorganization energy as:

  $$\lambda = \lambda_{in} + \lambda_{out} \tag{1.9}$$

  The first parameter, λ_{in}, is solvent-independent and it is related to the structural and geometrical differences of the inner shell between the reagent and product configuration.

$$\lambda_{in} = \frac{1}{2}\Sigma f_i(d_r^0 - d_p^0)_i^2 \quad (1.10)$$

The term f_i is a reduced force constant related to the inner sphere, d_r^0 and d_p^0 are the equilibrium bond coordinate of the reagents and product states. The equation is taken on all the significant intramolecular vibrations. The second term of (1.9) is a solvent reorganization energy, it considers the polarization and the organization of the surrounding molecules.

$$\lambda_{out} = (\Delta e)^2 \left(\frac{1}{2a_r} + \frac{1}{2a_p} + \frac{1}{r}\right)\left(\frac{1}{\epsilon_{op}} + \frac{1}{\epsilon_s}\right) \quad (1.11)$$

where (Δe) is the electronic change that is considered in the transfer, a_r and a_p are the radii of the reagents and donor shells those have a separation distance of r. ϵ_{op} and ϵ_r are the optical and static dielectric constant associated to the solvent.

- Harmonic oscillator model for the inner-sphere vibration

This model associates the complex of reagents and products as spheres under spring force that tends to restore the equilibrium with a force proportional to the displacement (Hooke law: $F = kx$).

This approach is applied in two previous values seen before: the reduced force f_i in the equation (1.10) and υ_n in the equation (1.8).

Particular attention is given to the second parameter υ_n, also called frequency factor. It represents a frequency of vibration that the system acquires to destroy the activated complex configuration assumed. It could be seen also as the frequency of overcoming the activation barrier. Formally it is written as the sum of all the mode harmonic frequencies υ_i that the system could assume:

$$\upsilon_n^2 = \frac{\sum \upsilon_i^2 E_i}{\sum E_i} \quad (1.12)$$

1.7 Electrochemical Kinetics and Sensors

The chemical basis of the work of the electrochemical sensors is the redox process that occurs between the target analyte and the device. A general redox process could be summarized by the equation:

$$R \rightarrow O + ne^- \quad (1.13)$$

R is the reduced state, O is the oxidated state and ne^- considers the number of electrons that are exchanged in the process.

The value of the redox potential is described by the Nernst equation:

$$E = E^0 + \frac{RT}{nF} ln \left[\frac{\prod_i a_{i,ox}}{\prod_j a_{j,red}}\right] \quad (1.14)$$

The parameters in (1.14) are: E^0 is the standard potential, R is the gas universal constant, T is the temperature, n is the number of electrons involved in the process, and F is the Faraday constant. The activities of the reduced and oxidated species are expressed by a_{red} and a_{ox}. Activities explain the behaviour of the ionic species in a complex system measuring the deviation with respect to the ideality. It is a value directly linked to the concentration of the species c through the activity coefficient f :

$$a = f\, c$$

In this way, it is possible to rewrite the Nernst equation in a more common way:

$$E = E^{0\prime} + \frac{RT}{nF} ln \left[\frac{C_{ox}}{C_{red}}\right] \quad (1.15)$$

where $C_{ox} = \prod_i c_{i,ox}$ and $C_{red} = \prod_i c_{i,red}$.

This equation is fundamental in the understanding of the process that occurs in an electrochemical sensor. Typically, this device is a system formed by three electrodes:

- Working electrode (WE): the main electrode responsible for the reception of the analyte through its active surface. Its material, or the material employed in its modification, is responsible for the effectiveness of the reaction. For this purpose, it is important to choose a good material that behaves in an electrocatalytic way with the analyte.

- Reference electrode (RE): it is the electrode used to control the potential applied to the working electrode. Considering that it is used as a reference it is important to present good stability. The most employed electrode are the Standard hydrogen electrode (SHE) and the silver/silver chloride (Ag/AgCl) one.

- Counter electrode (CE): it is responsible for the electron collection after the oxidation of the analyte that occurs on the working surface. For this purpose, it is usually employed a material that presents a good ohmic contact (metals such as platinum or gold). Through it, the current that is present in the solution is measured.

The system is linked to a Potentiostat to drive the redox reaction in the solution that in normal conditions should be not spontaneous. With overpotential, it is meant the “extra” potential that is applied to the system respects the standard potential of equilibrium of the Nernst equation:

$$\eta = E - E^0 \quad (1.16)$$

This parameter depends on compositional factors such as the material, the solution and the type of electrode employed. It is related to the internal energy organization of the system. From an energetic level point of view, the application of a potential of an electrode allows the shifting of the Fermi electron level of the electrode. the overpotential is the potential value that occurs when the electron Fermi level of the electrode coincides with one of the molecules in the solvent.

The over-potential related to the charge transfer is obtained through the Butler-Volmer equation. This equation represents the link between the potential applied to the systems and the current generated.

$$I = i_0 A \left(\frac{O_{el}}{O_{bulk}} e^{-\alpha \frac{nF\eta}{RT}} - \frac{R_{el}}{R_{bulk}} e^{(1-\alpha)\frac{nF\eta}{RT}}\right) \quad (1.17)$$

where i_0 is the exchange current density [A/m^2], A is the active surface of the electrode [m^2], α is the transfer coefficient, F is the Faraday constant, and η is the overpotential. The parameters O and R are referred respectively to the concentrations of the oxidised and reduced species. The subscript "el" denotes the concentration on the electrode surface and "bulk" refers to the concentration in the bulk.

The mechanism summarized by the Butler-Volmer equation follows this process:

- The electroactive species is immersed in the solvent and under an electric field they reach the electrode. In this step, the mechanism of mass transport and motion in the fluid plays an important role in determining the type of reaction that occurs.
- When the specie is approached to the electrode, the interaction and the electron transfer happen.

The entire mechanism is then dominated by two effects that characterize it: mass transport and electronic transfer. The mass transport could be assumed as the combination of diffusion, migration, and convection of the species in the solvent. The diffusion is the motion of material under a concentration gradient distribution. It is the dominant process in an electrochemical cell, and it is described by Fick's laws:

$$\Phi = -D \nabla C(x,t) \quad (1.18)$$

$$\frac{\delta C(x,t)}{\delta t} = D \nabla^2 C(x,t) \quad (1.19)$$

C expresses the concentration of the analyte in the solvent and D is the diffusion coefficient. The first Fick's law (1.18) defines the movement of the analyte due to differences in distribution and the second Fick's law (1.19) describes the behaviour of the concentration respect the time.

If we neglect the mass transport, we can assume that the concentration of the analyte in the solvent is homogeneous ($O_{el} = O_{bulk}$ and $R_{el} = R_{bulk}$) and it leads to the simplification of the Butler-Volmer equation :

$$I = i_0 A \left(e^{-\alpha \frac{nF\eta}{RT}} - e^{(1-\alpha)\frac{nF\eta}{RT}}\right) \quad (1.20)$$

In the Butler-Volmer equation is present also another important concept in electrochemistry: reversibility. It is associated with the losses and balance of the process between the anodic and cathodic currents. A process completely reversible is the idealized situation where the reactants are converted into products in a forward and reverse way without any losses. If the system starts to be affected by chemical change the process assumes the characteristics of a quasi-reversible process.

If the mechanism is irreversible, it means that the reaction is balanced completely in a specific direction (cathodic or anodic) and the other component is negligible. The degree of reversibility is associated with the dominant rate. In a reversible process, mass transfer is the determining step because it describes the species that can move in solution to guarantee the restoration of them. On the contrary, an irreversible process is dominated by the electron transfer rate.

1.8 Cyclic Voltammetry and Laviron equation

The cyclic voltammetry (CV) is the most famous technique used to characterize the electrochemical behaviour of determined species. It consists of a potential linear scan applied to the working electrode. Fixed a specific range the potential is applied cyclically to provide the electrochemical activation (meant as oxidation or reduction) of the analyte in the solvent. The resultant current that flows through the cell is measured with respect to the potential. It is a quantitative technique useful to estimate the presence and the amount of electrochemical species. It gives information also on the reversibility of the process and the behaviour of the molecules with the electrode.

The cyclic voltammetry provides a cartesian plot like the one presented in Figure 4. From the shape of the CV is possible to extract important values such as the peak current, the peak potentials, the half-wave potential and the peak width.

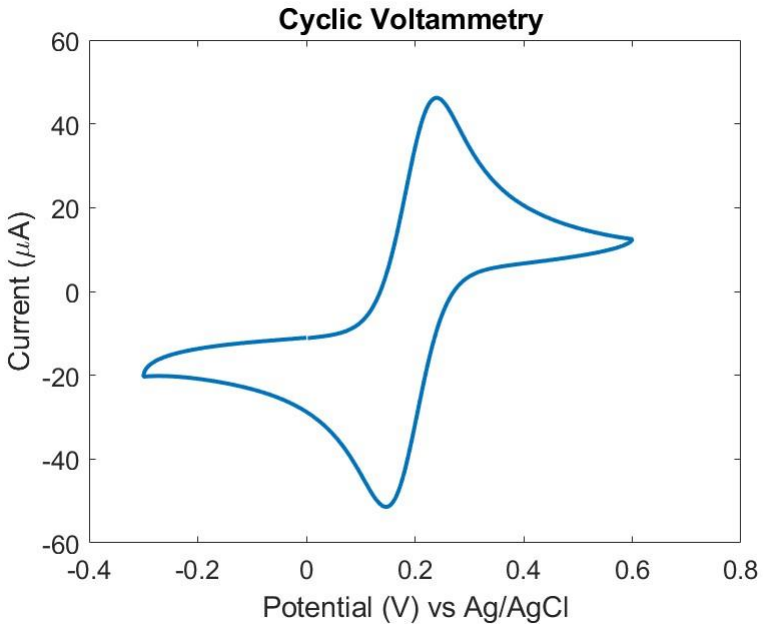

Figure 4 – Cyclic Voltammetry of 5mM of $K_4[Fe(CN)_6]$ in 0.1M KCl at scan rate of 100 mV/s

An important parameter that plays an important role is the scan rate ν (V/s) which determines the velocity of the potential change in time. It determines the behaviour of the analyte in proximity to the working electrode surface.

The impact of the scan rate on the peak current is described by the Randles–Ševčík equation:

$$i_p = 0.4663nFAC\sqrt{\frac{nF\nu D}{RT}} \tag{1.21}$$

Where n is the number of electrons exchanged in the redox reaction. From the equation, it is possible to analyse the diffusion coefficient D and the effective area surface of the working electrode A. The peak current, as expressed in the formula, increases with the square root of the scan rate ν. This is related to the fact that a high value of scan rate does not allow the expansion of the diffusion layer and a large concentration gradient occurs near the electrode surface. The Randles–Ševčík equation is valid only for reversible processes because in its derivation it is assumed that the oxidation current density and the reduction one are equal in modulus $j_{ox} = |j_{red}|$.

To calculate some important parameters like the electron transfer constant k or the electron transfer coefficient α, in 1979 Laviron developed a theory to study the electrochemical behaviour of electroactive species in a cell [59]. From this model, the electron transfer coefficient α is obtained from the slope of the plots of the potential peak position with respect to the logarithm of the scan rate. The slopes (m_c is related to the regression line of the cathodic peaks and m_a to the anodic one) are considered equal to:

$$m_c = -\frac{2.3\,RT}{\alpha nF} \tag{1.22a}$$

$$m_a = \frac{2.3\,RT}{(1-\alpha)nF} \tag{1.22b}$$

Where n is the number of electrons exchanged in the redox process. Replacing the value of the slopes and simplifying the equation, it is derived the equation:

$$\alpha = \frac{m_a}{m_a - m_c} \tag{1.23}$$

The electron transfer rate k is calculated through the following equation

$$log(k) = \alpha log(1-\alpha) + (1-\alpha)log\alpha - log\left(\frac{RT}{nF\nu}\right) - \alpha(1-\alpha)nF\left(\frac{\Delta E_p}{2.3RT}\right) \tag{1.24}$$

It is important to remark that the previous equations are valid only if is verified the condition $n\,\Delta E_p > 200\,mV$.

1.9 DLVO Theory and Lennard-Jones Potential

To treat the behaviour of colloidal particles in a liquid medium Boris Derjaguin, Lev Landau, Evert Verwey and Theodoor Overbeek formulated the so-called DLVO theory, an acronym of their names. The concept focuses attention on the interaction and the resulting stability of the aggregates [60]. They consider two main forces acting in the system: The electrostatic force and the Van der Waals one. The first is the result of the electrostatic interaction between charged particles that could lead to repulsion in the case of particles of the same charge or attraction if the particles have opposite charges.

The Van der Waals theory of forces treats the interaction in intermolecular systems. This type of force could be well explained by the Lennard-Jones potential in the DLVO framework [61]. The mathematical model of Lennard-Jones explains the interaction between two atoms or molecules in terms of repulsive and attractive forces and is resumed in the formula:

$$V(r) = 4\varepsilon\left[\left(\frac{\sigma}{r}\right)^{12} - \left(\frac{\sigma}{r}\right)^{6}\right] \tag{1.25}$$

where r is the generic particle distance, ε is the depth of the potential well and σ is the particle distance configuration at which the potential is zero.

The model is called also the '12-6 law' from the expression of the formula that consists of two terms:

- The repulsive one: $\left(\frac{\sigma}{r}\right)^{12}$, the term dominates when the two particles are very close to each other and represents the repulsive force due to the overlap of the electron clouds (due to the Pauli exclusion repulsion)
- The attractive one: $\left(\frac{\sigma}{r}\right)^{6}$, it is the representation of the Van der Waals attraction force that dominates at intermediate distances. It is related to dipole-dipole interaction and London dispersion forces when the particles are not too close or too far from each other.

The graphical representation of the potential force between two particles with respect to their distance is shown in Figure 5.

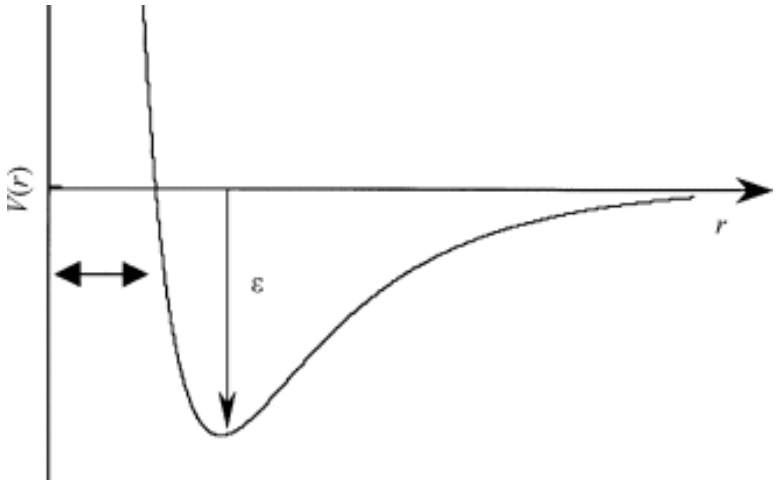

Figure 5 – Lennard Jones potential

A surfactant is a molecule that reduces the interfacial tension increasing the wettability between a solid and a liquid. In a synthesis process, it could influence the stability of a colloidal system playing a specific role in the DLVO framework. The surfactant could be adsorbed onto the surface of colloidal particles by physisorption creating a sort of shield in the structure [62]. This phenomenon leads to a reduction in Van der Waals forces between particles preventing them from aggregating and precipitating in the solution. In the graphical representation of the Lennard-Jones potential, the action of a surfactant helps to reach the minimum of the potential, where the particles tend to organize at the more stable distance configuration.

1.10 Project Aim

This project has as its main object the study of the electrochemical behaviour of biological molecules such as paracetamol, dopamine, and uric acid. These molecules

have a lot of attention due to their toxicity at high concentrations and due to their direct link with disease diagnosis. This is the reason for the importance of developing techniques and materials to improve performance and to find the best trade-off for each application. Bismuth has been presented as a powerful material that is under study as an electrocatalyst in electrochemical detection. Also, the role of the Polyethylene glycol used as a surfactant in bismuth structure synthesis is studied. Validated from the theoretical framework of DLVO, the change of geometry and improvement in electrochemical detection are investigated.

2 Materials and Methods

2.1 Synthesis

The starting point of the synthesis process is inspired by the work of Liu et al. [63]. Subnitrates bismuth composites were produced by a simple stirring process. The precursor used was the bismuth (III) nitrate pentahydrate, $Bi(NO_3) \cdot 5H_2O$, which was dissolved in butanol ($C_4H_{10}O$) with a ratio of 1:12, as it is shown in Table 1 –The mixing was carried out using a sonication tip for 1 hour to reach a semi-homogeneous suspension. The stirring procedure was composed of two alternating steps: 20 seconds of mixing and 10 seconds of rest to avoid the temperature increase and unwanted reactions.
A drying step followed in an oven at 150° until complete evaporation of the butanol. At the end of the synthesis, the product obtained was $HO - BiONO_3$.

Other products were synthetized adding different concentrations of polyethylene glycol (PEG) in different weight ratios respect the $Bi(NO_3) \cdot 5H_2O$ used.

All the materials were labelled BPX where 'X' refers to the PEG/Bismuth ratio used in the synthesis.

Product	$Bi(NO_3) \cdot 5H_2O$	Butanol	PEG
BP0	5 mg	60 mL	0 mg
BP1	5 mg	60 mL	5 mg
BP2	5 mg	60 mL	10 mg
BP4	5 mg	60 mL	20 mg
BP8	5 mg	60 mL	40 mg

Table 1 – Material preparation for the synthesis

Before the mixing procedure with the sonication tip, all the materials were ground in a mortar to obtain the finest possible powders to add to the butanol.

All the products in which PEG was used were washed several times in ethanol with the use of a microcentrifuge to remove the excess of PEG.

The materials used in this project have been provided by Sigma Aldrich (US).

2.2 Solution Preparation

The analytes used in this project are paracetamol, dopamine, and uric acid. As the electrolyte used to study the sensing of the previous analytes was chosen the Phosphate Buffer Saline (PBS) because of its ion concentration and pH regulation, which is very similar to the human body condition.

Some tablets of PBS purchased by Sigma Aldrich were dissolved in deionised water (DI) and then each analyte was added with the appropriate weight to obtain the desired molarity.

Final molarity	**Weight**	**PBS volume**
5mM Paracetamol	37.79 mg	50 mL
5mM Dopamine	47.41 mg	50 mL
5mM Uric Acid	25.22 mg	30 mL

Table 2 – Solution preparation

All the other concentrations were obtained through successive dilutions. The storage of the solution after its preparation requires particular attention[64]. For the paracetamol and UA solution storage, it is not evident the short-term degradation, and the solution was kept in normal conditions at pH 7.4. Dopamine is a light-sensitive molecule, and the neutral pH of the PBS induces the degradation effect of the solution. Several publications have demonstrated the decomposition of the dopamine solution after 24/48h after the dilutions [65]. To avoid the risk of degradation, dopamine solutions were stored in a fridge at 4°C covered by an aluminium foil.

2.3 Electrode Modification

Thanks to the help of screen-printing technologies, it is possible to realize a three-electrode system embedded on a plastic or ceramic substrate. In Figure 6 - (a) it is shown the screen-printed electrode (SPE) fabricated by Metrohm DropSens. The schematic representation of the three-electrode system is presented in Figure 6 – (b). The strip provided by Dropsens was used as an electrochemical cell at three electrodes: the reference, the working and the counter one. The working electrode has a circular surface (4mm of diameter) and it is made of carbon as the counter electrode, while the reference electrode is made of Ag.

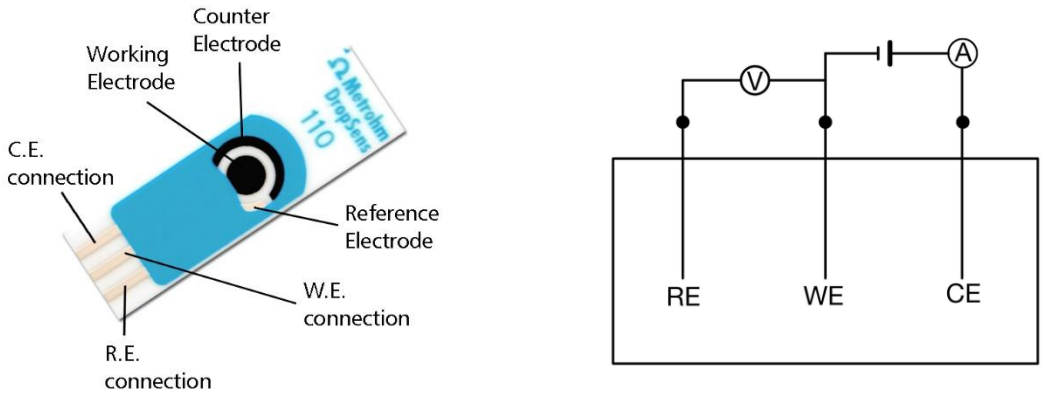

(a) (b)

Figure 6 – Three-electrode sensor: (a) SPE 110 by DropSens and (b) its schematic structure

The strip was used as an efficient structure in sensing all the studied analytes. Considering the aim of the research, the working electrode was modified to appreciate the electrocatalytic work of all the Bismuth-based material studied. The modification of the working electrode could be performed in different ways: electrodeposition, chemical deposition and so on. The technique used in this case was drop-casting, a simple and easily manageable procedure that involves the mechanical deposition of a solution drop on the working electrode through the use of a mono-channel pipette.

Following the procedure used by Liu et al. [63] the solution employed was a mixture of 3 mg of bismuth-based powder added in 1 mL of deionized water. The solution was mixed in a sonication bath for 30 minutes until a homogeneous suspension was reached.

Then 5 µL of the solution prepared was deposited on the working electrode and left overnight to allow the evaporation of the water. During the procedure, particular attention was paid to the deposition of the drop on the working avoiding the expansion of the drop on the other two electrodes. In particular, the deposition on the counter electrode of the bismuth structure could affect the collection of electrons during the CV. It is not a remarkable problem such as the unwanted deposition of bismuth on the reference electrode, that could affect the analysis of the position of the peak due to a potential shift. This could be a problem in the electrokinetic study of the sensor but also in the comparison with the others.

2.4 Electrochemical Measurement Setup

Each analyte (paracetamol, dopamine, uric acid) has been studied through the CV technique.
The parameters employed in every analysis are shown in Table 3. For the electrochemical study based on the Laviron theory, different voltammetry was

performed with different scan rates between 50 mV/s and 250 mV/s with steps of 50 mV/s. For the comparison between the different electrodes, a common condition of 1 mM of analyte with a scan rate of 100 mV/s was employed.

ANALYTE	Upper potential (V)	Lower potential (V)
Paracetamol	0.9	-0.3
Dopamine	0.6	-0.1
Uric Acid	0.7	0

Table 3 – Potential ranges employed in Cyclic Voltammetry

In Figure 7 the cyclic voltammetry setup is shown with the SPE linked to the potentiostat. The latter is an AUT302N.MBA.S and it is provided by Autolab Metrohm. The end of the apparatus is represented by the Data Acquisition system to collect and visualize in real-time the results of the measurements.

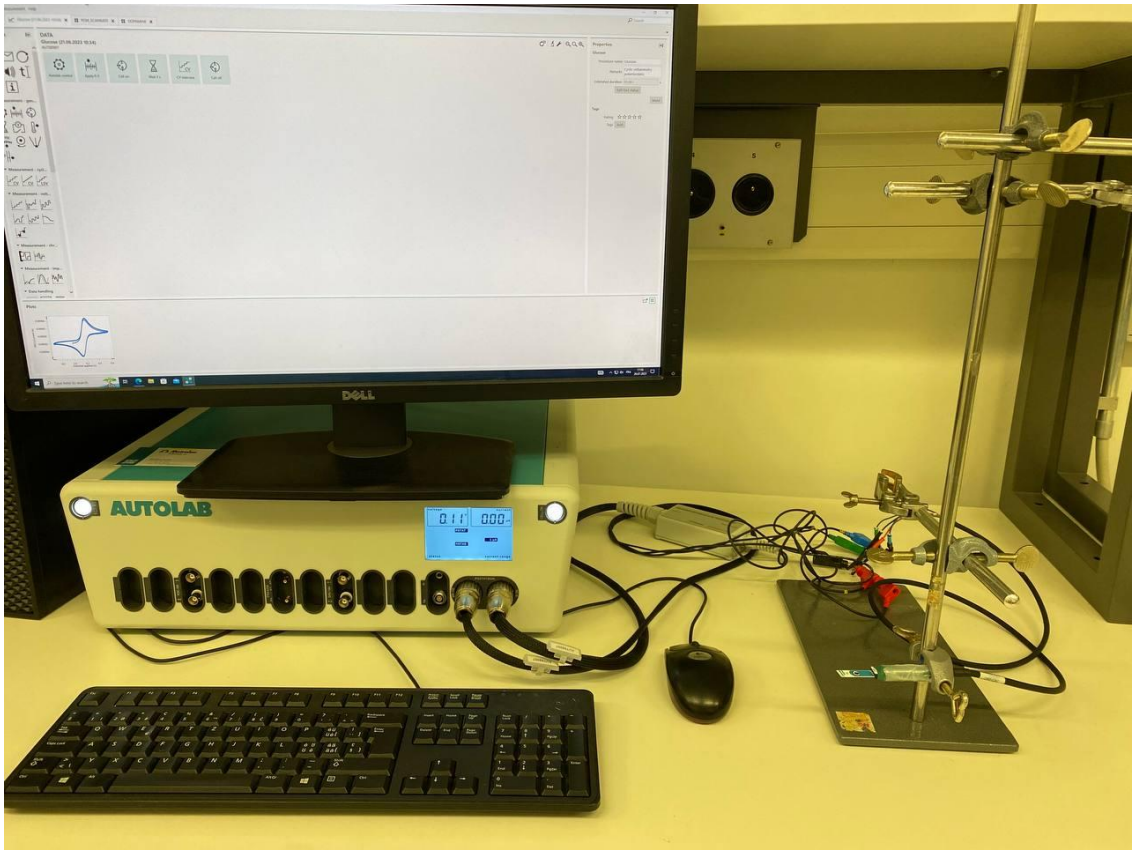

Figure 7 – Electrochemical measurement setup

3 Material Characterization

3.1 Raman Spectroscopy

Raman spectroscopy is a powerful tool that allows to check the material composition and to study the crystallography composition of the sample.

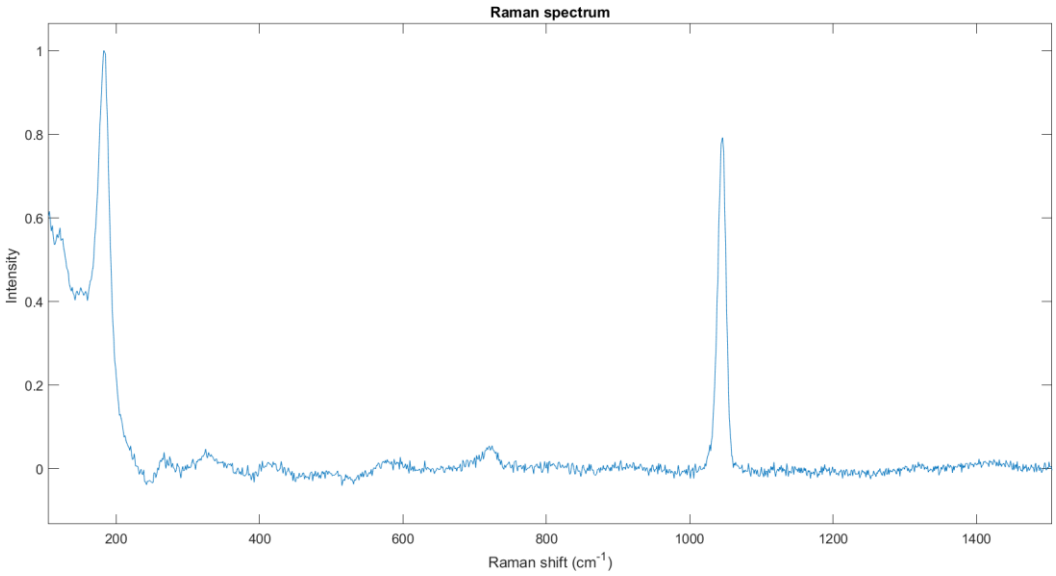

Figure 8 – Raman spectrum BP0 sample

Figure 8 shows the BP0 Raman spectrum sample. It shows the presence of the nitrate group represented by the peak in $1046\ cm^{-1}$, confirmed also by the work of Mabrouk et al. [66] that clear the specificity of that peak for the nitrate group NO_3.

The other peak in $182\ cm^{-1}$ represents the stretch between the $Bi - O$ bond of the molecule as enlightened in [67] where Bismuth compounds are analysed. Also from [42] it is possible to conclude that the structure obtained is a $HO - BiONO_3$ due to the slight temperature increase of the stirring procedure, approximately 100° C. For all the other samples it is difficult to perform the Raman analysis due to the presence of the PEG in the compounds despite the washing. However, it is possible to conclude that the presence of the PEG does not alter in a significant way the composition of the compound that still may present a bismuth subnitrate structure.

3.2 IR Spectroscopy

Considering that through Raman spectroscopy it is not possible to study the composition of the PEG-based synthesized material, an IR analysis is presented. With

this analysis, it is possible to study preliminarily the composition of the samples and to make assumptions about them.

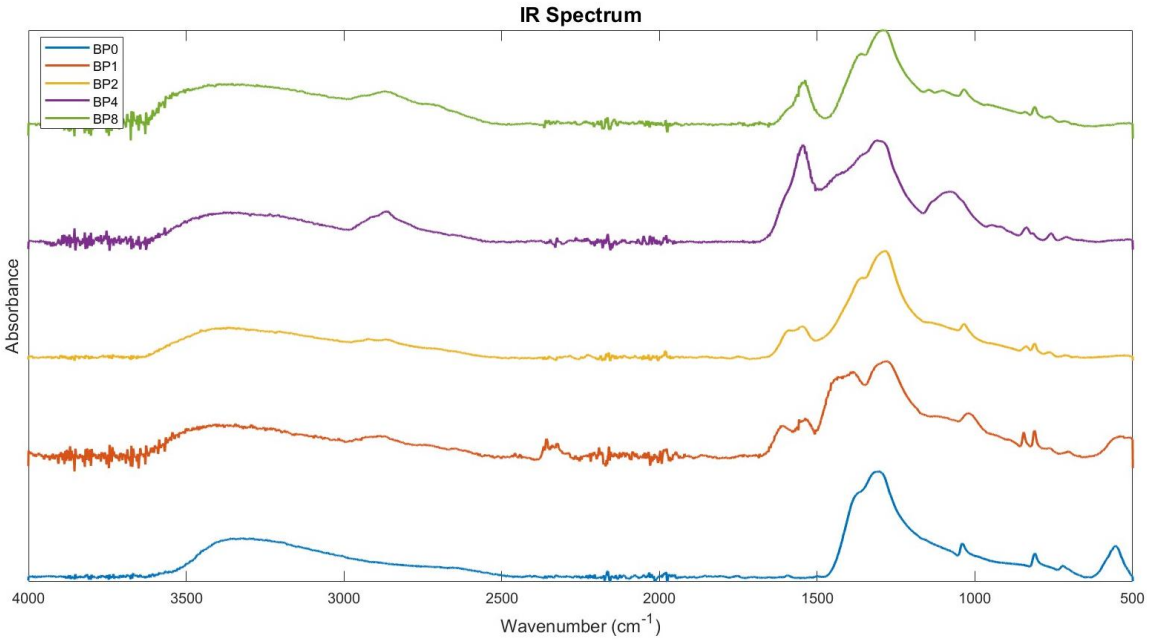

Figure 9 – IR spectrum of the samples

From Figure 9 it is possible to link each obtained peak to a vibrational bond of the atomic composition of the samples. With the comparison between the BP0 (without the use of the PEG during the synthesis) and the other samples, it is possible to understand if the PEG is present in the composition. The peak at $3500 - 3200\ cm^{-1}$ is related to the HO bond on the surface of composites, that it is present in the BP0 spectrum as the theories predict, but it is also present in the PEG-based composited that could confirm the presence of the hydroxy group in the external molecule composition. The peak between $1350 - 1250\ cm^{-1}$ is corresponding to the strong absorption peak of NO_3^- and the small peak around $1000\ cm^{-1}$ is related to the Bi-O bond.

Even though the PEG-based samples have been subjected to washing procedure, it is possible that in the microstructure of the samples, some PEG compound remains in the structure. It is validated by the fact that there is a small peak around $2900\ cm^{-1}$ related to the C-H bond of the PEG, particularly in the BP4 structure. From the spectrum, it is interesting to notice the peak around $1650 - 1500\ cm^{-1}$. This peak is completely absent in the BP0 spectrum, and it increases passing from BP1 to BP4. From the literature, it could be related to the N-O bond or the C-O bond. It could be assumed to be a specific configuration of the molecular structure or still to the presence of the PEG compounds present in the sample.

3.3 Optical Microscopy

The use of optical microscopy allows to appreciate the morphology of the modified electrode through the Bismuth-based samples. This analysis is not as accurate as a scanning electron one, but it gives a rough idea of the modified surface structure of the electrode at the microscopic level.

Figure 10 shows how the working electrode (area of $0.12\,cm^2$) appears after the modification. All the electrodes appear different because in the modification process, the precision of the drop deposition is delicate. Some other conditions could affect the appearance of the electrode, such as the solubility of the material in the water, the time of evaporation after the drop-casting and the temperature.

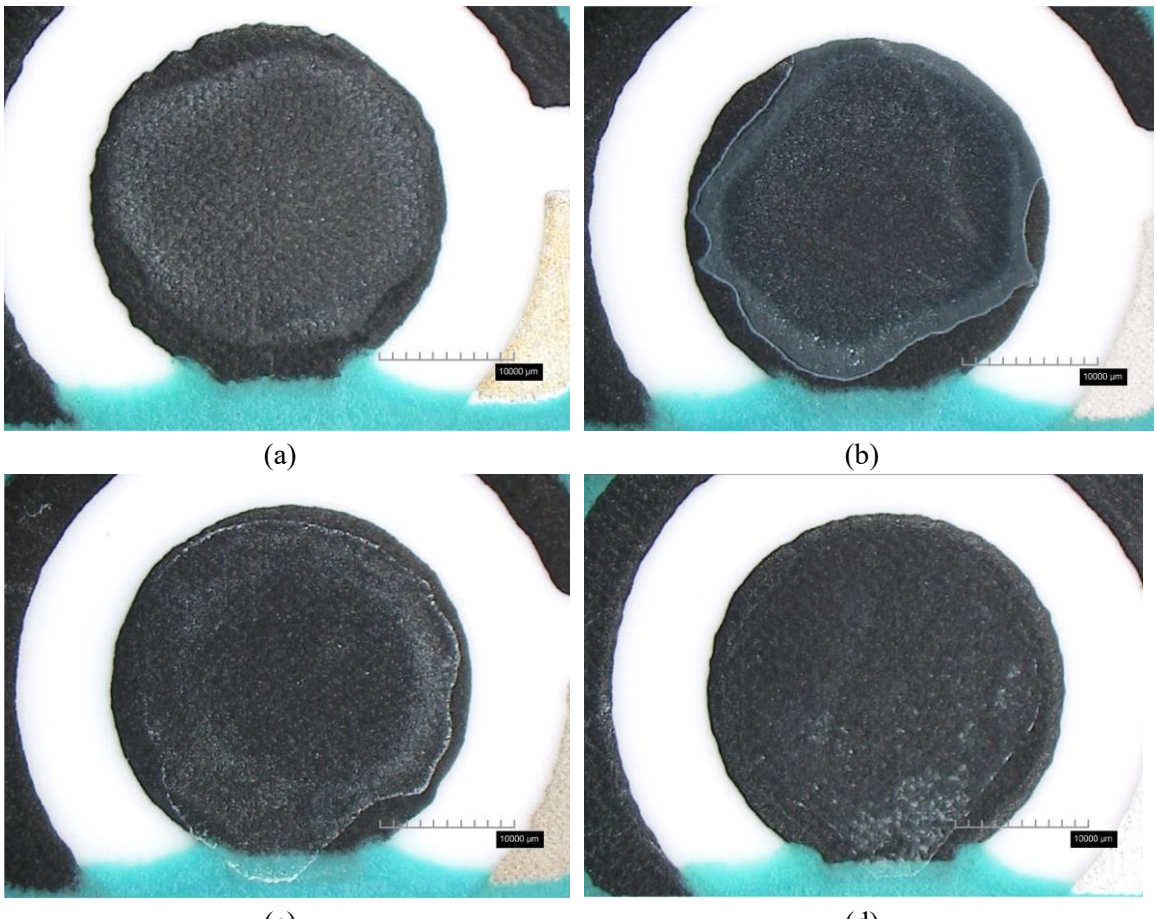

(a) (b)

(c) (d)

Figure 10 – Optical microscope images of the modified working electrode: (a) BP0, (b) BP1, (c) BP2, (d) BP4

With the use of the optical microscope, the image has been magnified as shown in Figure 11. It is possible to appreciate the presence of the bismuth materials on the top of the electrode and at first hypothesis, the BP4 working electrode presents a rougher structure that could lead to a greater surface area. This is only the first analysis, that could be validated only by SEM spectroscopy.

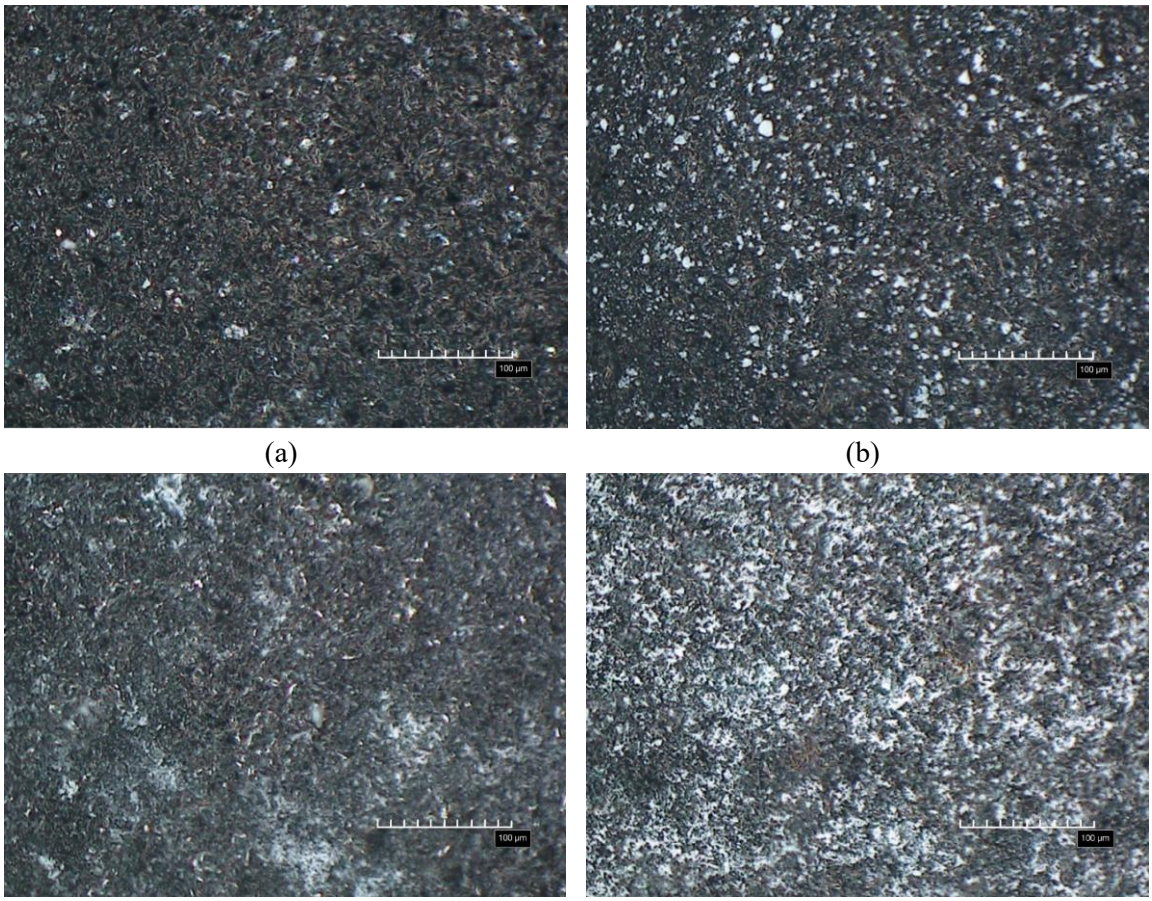

(a) (b)

(c) (d)

Figure 11 – Optical microscope magnification (100µm bar) images of the modified working electrode: (a) BP0, (b) BP1, (c) BP2, (d) BP4

3.4 Scanning Electron Microscopy

A further study of the sample used to modify the electrodes is given by a Scanning Electron Microscopy (SEM) analysis. An electron gun was used with an electron energy of 5 keV. The collected images derive from the collected secondary electron to have a better spatial resolution and highlight differences in the morphology of the microstructures [68]. It is highlighted that for the measurement a Field Emission Scanning Electron Microscope (FESEM) was employed. It is a particular type of SEM that uses a sharp tip to generate a smaller and coherent electron beam which leads to higher resolution also at the nanoscale.

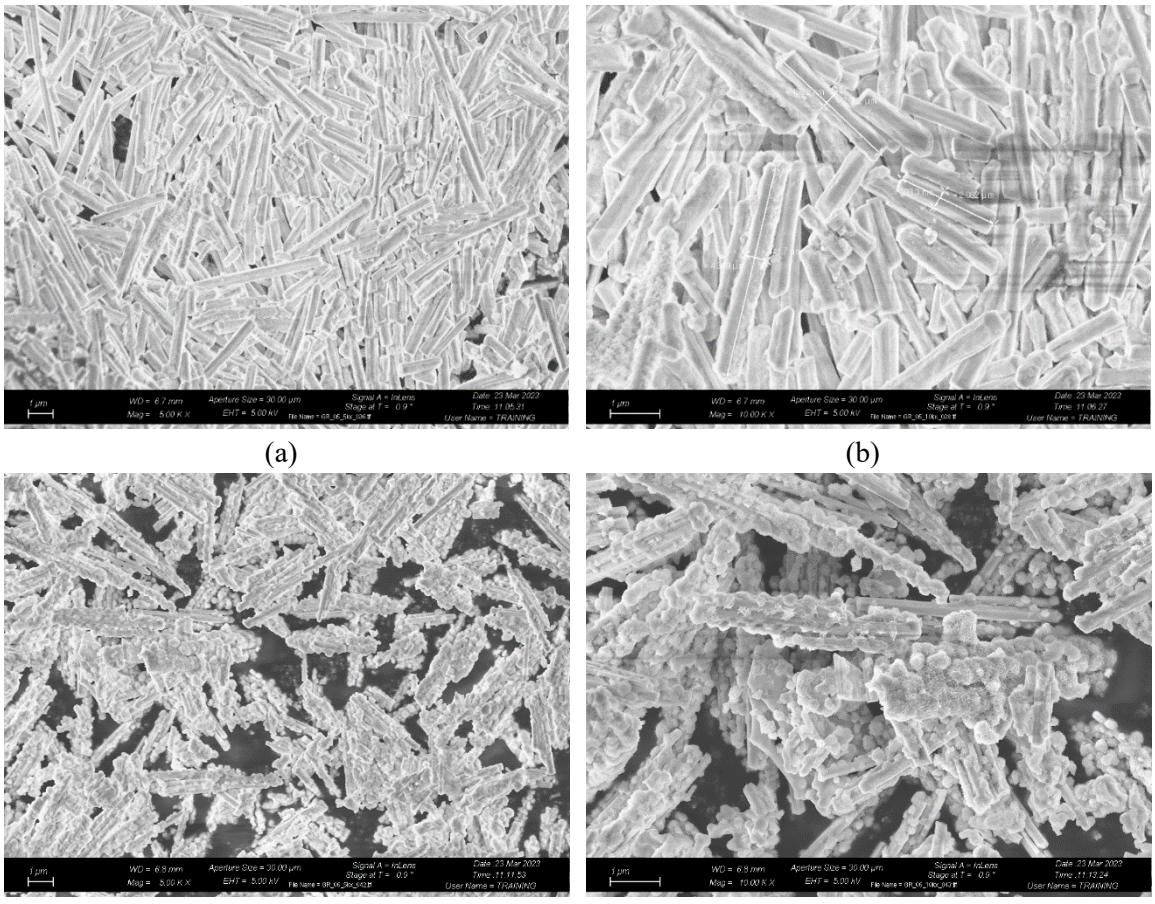

(a) (b)

(c) (d)

Figure 12 – SEM images of the samples: (a) BP2 mag. 5k, (b) BP2 mag. 10k, (c) BP4 mag. 5k, (d) BP4 mag. 10k

The structure of BP2 presented in Figure 12-(a) is composed by micrometric rods with a small amount of nanometric features on its surface that appear quite rough. Particularly interesting is the SEM acquisition of the BP4 presented in Figure 12-(c) and Figure 12-(d). The surface appears complex in terms of morphology. A further magnification is performed in order to appreciate better the smallest features of the structure and the results are shown in Figure 13 – (b).

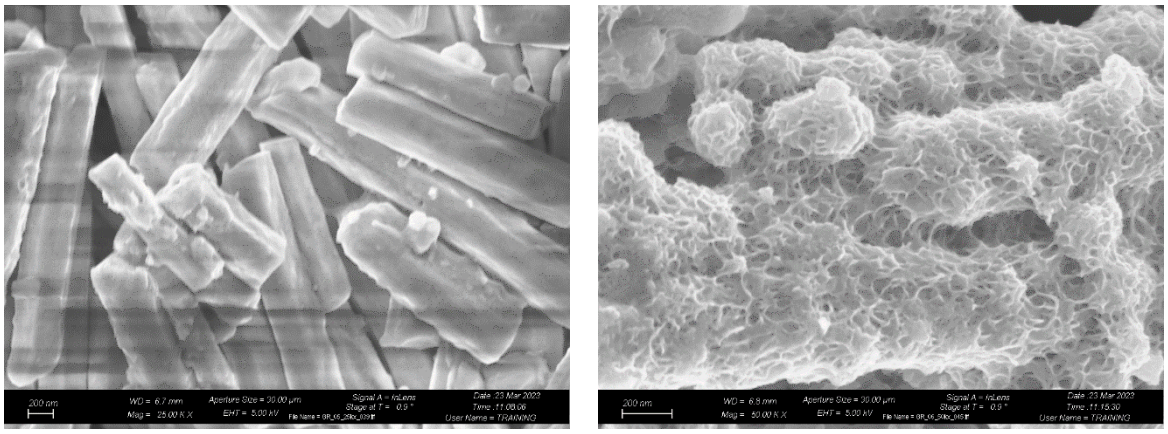

(a) (b)

Figure 13 – SEM images of the samples: (a) BP2 mag. 25k, (b) BP4 mag. 50k,

The presence of this rough surface could be related to the high stability due to PEG during the synthesis process. The surface presents nanometric features that increase the surface-to-volume ratio of the entire structure. This morphology could be related to an improved electrocatalytic action that must be validated by an electrochemical analysis.

4 Results and Discussion

4.1 Electrochemical Impedance Spectroscopy

Electrochemical impedance spectroscopy (EIS) is a technique used to evaluate the interfacial electron-transfer properties in an electrochemical cell. It involves the application of a sinusoidal signal to generate a perturbation in the system. The AC perturbation is applied to the working electrode over a determined range of frequencies. The impedance is calculated from the ratio of the current generated by the process and the voltage [69]. The main advantage of this technique is that it is not a destructive method that keeps the system in the equilibrium state. It studied the charge transfer resistance of all the SPEs by dropping 100 µL of 0.1 M PBS containing 5 mM $Fe(CN)_6$on the surface of the electrodes. The bias potential was fixed at 200 mV, and the alternating current voltage was 10 mV with a frequency in the range of $[10^{-1} - 10^5]$ Hz.

The generated result is the Nyquist plot, shown in Figure 14, where the real and the imaginary part of the impedance are represented. The semicircle shapes obtained provide information on the resistance values of the system.

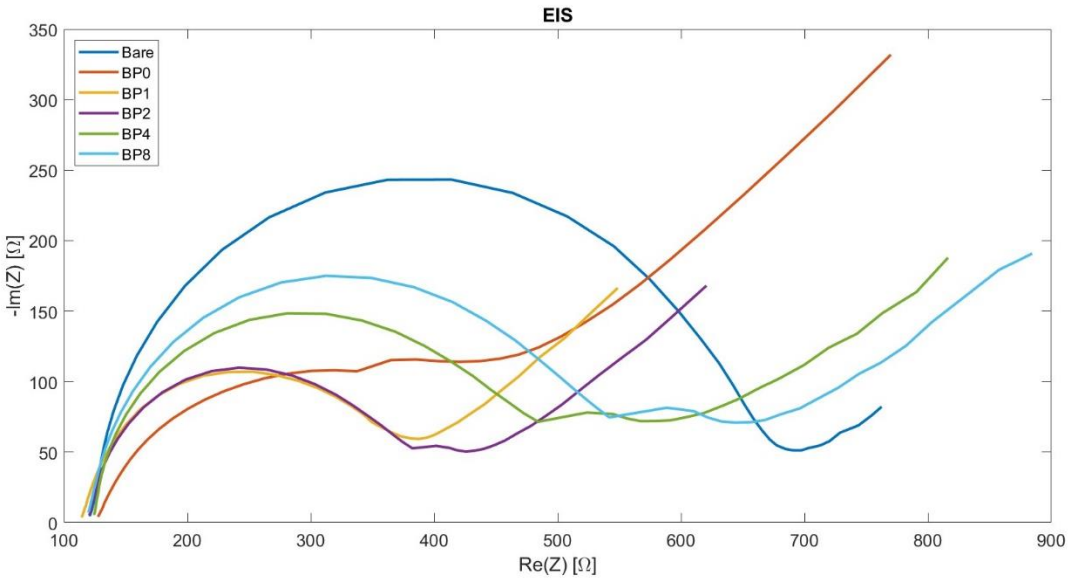

Figure 14 – Nyquist plot of the electrode EIS analysis

Figure 15 presents the sketch of circuital configurations of the system, where R_s is the resistance of the electrolyte, known as 'uncompensated resistance'. At the interface between the working electrode and the solution the electric double layer formed could be considered as the parallel of capacitor C and resistor R_i. The results obtained are summarized in Table 4.

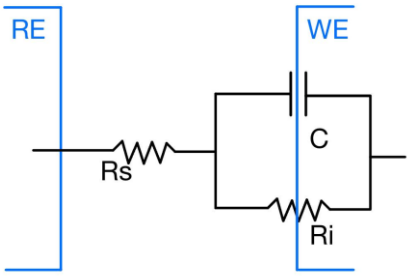

Figure 15 – Electric model at the interfaces

ELECTRODE	R_i (Ω)
BARE	569.6
BP0	209.7
BP1	266.4
BP2	271.7
BP4	325.7
BP8	422.0

Table 4 – Electrodes Interfaces Resistances

The uncompensated resistance is almost equal for all the electrodes and has the value of 121.2 Ω while the value of the interface resistance R_i feels the influence of the surface modification of the electrode. Indeed, the bare electrode presents the highest resistance of 569.63 Ω and all the modified electrodes have smaller values due to the electrocatalytic properties of the bismuth and a reduced resistivity respect to the carbon surface of the working electrode. It is interesting to notice also that the value of the interface resistance R_i follows the amount of PEG used in the synthesis of the material. It could be associated with some molecules of the surfactant still present in the

microstructure. Those molecules act as a barrier at the interface and increase the value of the resistance.

4.2 Cyclic Voltammetry – Paracetamol

Each analyte was studied through cyclic voltammetry analysis. The potentiostat was linked to the screen-printed electrode (Dropsens 110 strip) to create all the connections needed for the analysis. With the use of a micropipette 100 µL of solution is dropped on the electrodes. Then different scan rates and concentration measurements were performed to study the electrochemical kinetics of the sensors and their sensitivity.

4.2.1 Paracetamol – Kinetic Characterization

Paracetamol [PCM] goes under electrochemical oxidation by electrolytic etching of the aromatic ring through a two-electron process [70]. The final product is the N-acetyl-p-quinoneimine and the process is shown in Figure 16.

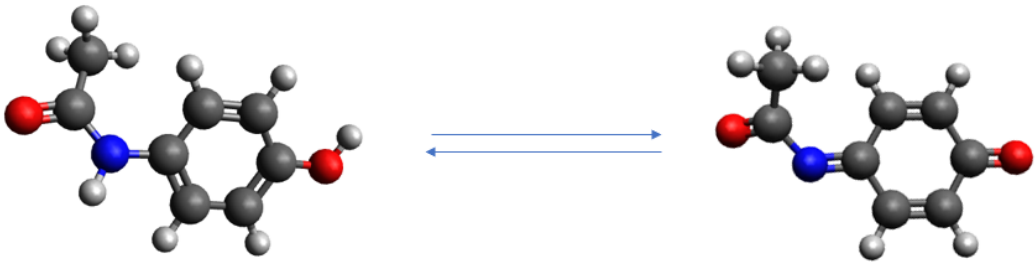

Figure 16 – PCM – Mechanism of electrochemical oxidation [Avogadro® optimization]

The electrochemical activity of paracetamol was validated by performing a cyclic voltammetry with an unmodified SPE. It was compared with the behaviour of the electrodes if a solution of only PBS was dropped on it as represented in Figure 17.

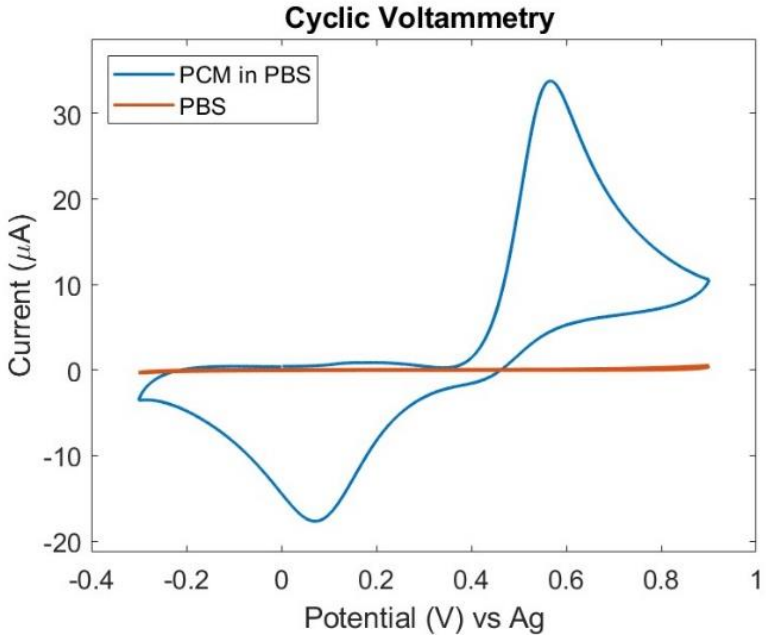

Figure 17 – PCM – Cyclic Voltammetry of 1mM paracetamol in 0.1M PBS compared with blank solution of PBS

As it is observed in the previous figure the presence of paracetamol in the solution is related to the presence of oxidation and reduction peaks in the obtained plot, therefore it is possible to study the behaviour of the peaks in different situations to characterize the electrode. It is important to underline the fact that every voltammogram reported has been baseline-corrected in order to avoid capacitive or parasitic current and to analyse only the faradic one.

Each measurement was performed 3 times to obtain the standard deviation of the results. It is important to remark that the process of cyclic oxidation and reduction of the materials on the electrode could cause the formation of other molecules that could remain detached on the surface and interfere with successive. For example, the process of the oxidation of paracetamol in NAPQI could generate some molecule that remains in contact with the working electrode and makes more difficult the reduction of NAPQI. This is the reason that after every measurement each sensor is cleaned several times with distilled water and let dry in air before the successive cyclic voltammetry.

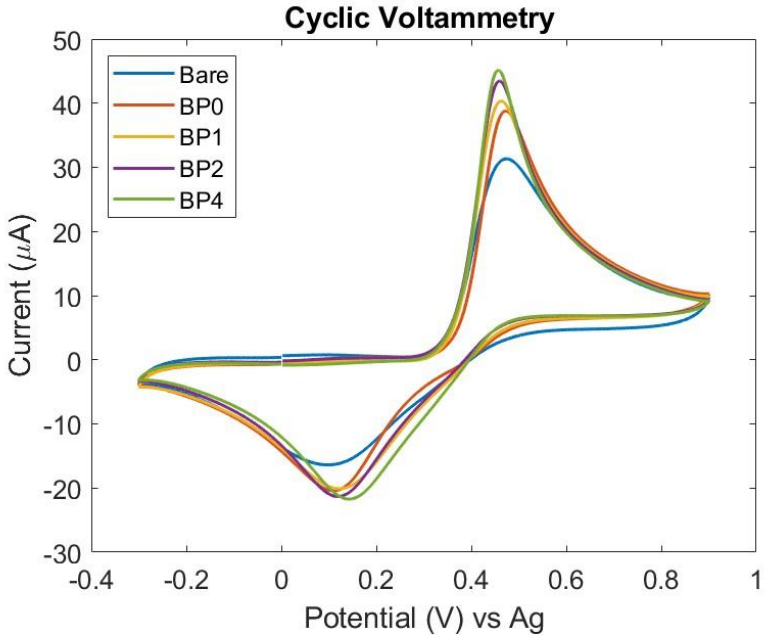

Figure 18 – PCM - Comparison between the bare electrode and the modified ones. Concentration of paracetamol 1mM in 0.1M PBS at scan rate of 100mV/s

In Figure 18 all the cyclic voltammetry measurements are presented showing the comparison between the performance of the bare electrode with respect to the ones of the modified sensors. The concentration of paracetamol is 1mM in an electrolytic solution of 0.1M PBS at a scan rate of 100 mV/s. The electrocatalytic behaviour of the Bismuth is confirmed. All the peaks of the modified electrodes are higher and more marked. This is due to the activity of the bismuth that plays the role of mediator in the electron transfer between the paracetamol and the carbon working electrode. Also, the modified electrode performance is related to the process of formation of the bismuth aggregates. Indeed, the presence of PEG in the synthesis of material increased the stability leading to an increase of the surface area of the obtained material. An increase in the surface area is related to an increase in the active area that represents all the possible "paths" for the electron to reach the electrode and perform the electron transfer.

In Table 5 the oxidation peak currents are presented. It shows that the value of the current increases if the electrode is bismuth-modified and if more PEG was used in the synthesis process.

ELECTRODE	$I_{pa}(\mu A)$
BARE	31.09 ± 1.57
BP0	38.79 ± 1.77
BP1	40.83 ± 1.59
BP2	43.46 ± 2.83
BP4	45.16 ± 1.56

Table 5 – PCM - Oxidation Peak Currents

The peak current is the first parameter analysed that represents the first validation of the electrode performance. For a more complete and deeper analysis, the use of the Laviron model is needed to find the electron transfer coefficient α and the kinetic constant rate k.

ELECTRODE	ΔE_P (mV)	α	D(cm^2/s)	Rate constant k (ms^{-1})
BARE	446 ± 31	0.46 ± 0.14	$1.39 \cdot 10^{-6}$	0.69 ± 0.29
BP0	392 ± 11	0.46 ± 0.06	$2.03 \cdot 10^{-6}$	1.60 ± 0.40
BP1	379 ± 17	0.45 ± 0.08	$2.13 \cdot 10^{-6}$	2.77 ± 0.74
BP2	367 ± 13	0.45 ± 0.16	$2.45 \cdot 10^{-6}$	5.36 ± 0.66
BP4	354 ± 18	0.44 ± 0.12	$2.62 \cdot 10^{-6}$	5.72 ± 0.67

Table 6 – PCM - Kinetic parameters of different SPEs

In Table 6 all the calculated parameters are shown. ΔE_P represents the potential distance between the two peaks in the voltammogram. The diffusion coefficient D is calculated from the peak current and inverting the Randles-Sevcik equation. The transfer coefficient is evaluated by plotting the position potential of the peaks with respect to the logarithm of the scan rate. By using the Laviron model and the equation (1.24), the rate constant is calculated.

It is interesting to notice that the PEG-synthesized materials have an impact on the electrochemical properties. Indeed, the increasing use of the PEG in the process is related to a decrease of ΔE_P and α and an increase of D and k. Particularly interesting is the last one, the rate constant k which determines how an electrochemical process is fast and effective. The measurements have shown that the modified electrodes employed present 7-8 times higher values of the rate constant with respect to the bare electrode.

To check the freely diffusing RedOx species interaction with the SPE different measurements were performed by checking the scan rate. It is varied from 50mV/s to 250 mV/s and according to the Randles-Sevcik equation the peak current increases with the square of the scan rate as shown in Figure 19 for the bare electrode.

The same procedure was performed for all the other modified SPEs to appreciate the behaviour of the sensor for different scan rates. The results obtained are shown in Figure 20 for BP0, Figure 21 for BP1, Figure 22 for BP2, and Figure 23 for BP4.

Linear regression current equations and their regression coefficients are shown in Table 7 and linear regression peak potential equation in Table 8.

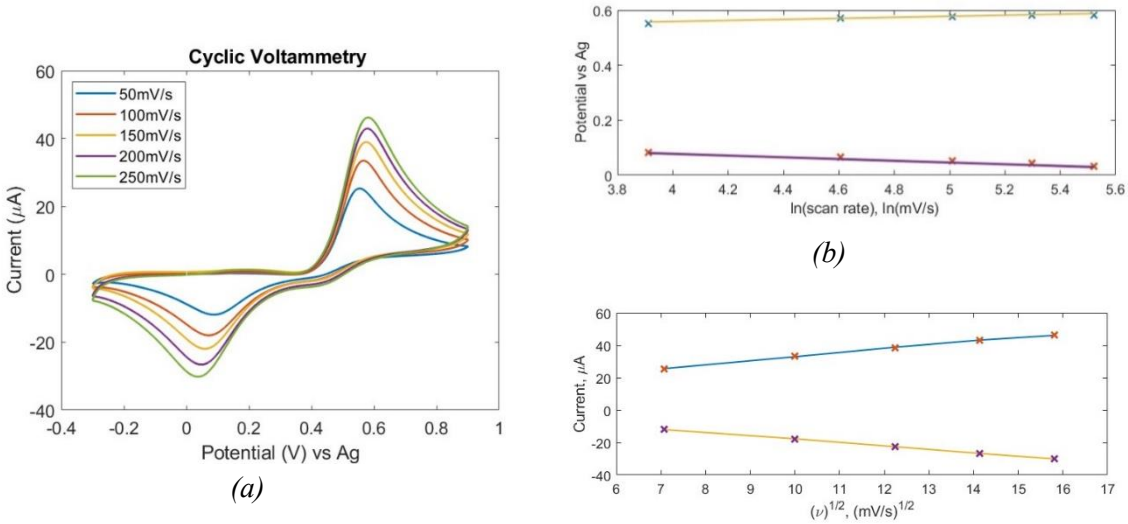

(a) *(b)* *(c)*

Figure 19 - (a) Cyclic voltammetry for the detection of 1mM of paracetamol in 0.1M PBS with a Bare electrode, change in the scan rate from 50 mV/s to 250 mV/s, (b) dependence of the positions of the potential peaks respect the logarithm of scan rate, (c) dependence of the current anodic and cathodic peaks respect the square root of the scan rate

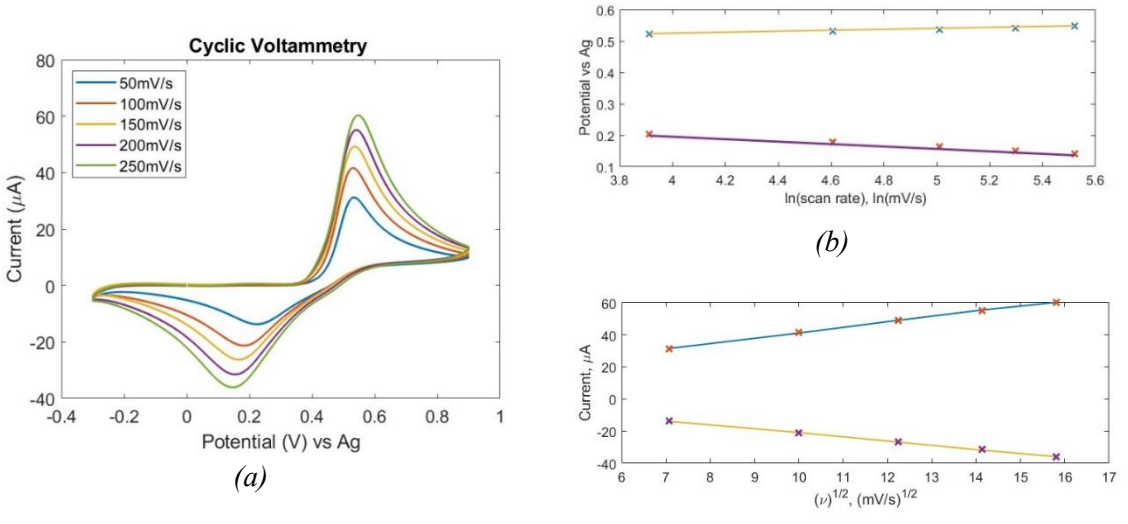

(a) *(b)* *(c)*

Figure 20 - (a) Cyclic voltammetry for the detection of 1mM of paracetamol in 0.1M PBS with a BP0 electrode, change in the scan rate from 50 mV/s to 250 mV/s, (b) dependence of the positions of the potential peaks respect the logarithm of scan rate, (c) dependence of the current anodic and cathodic peaks respect the square root of the scan rate

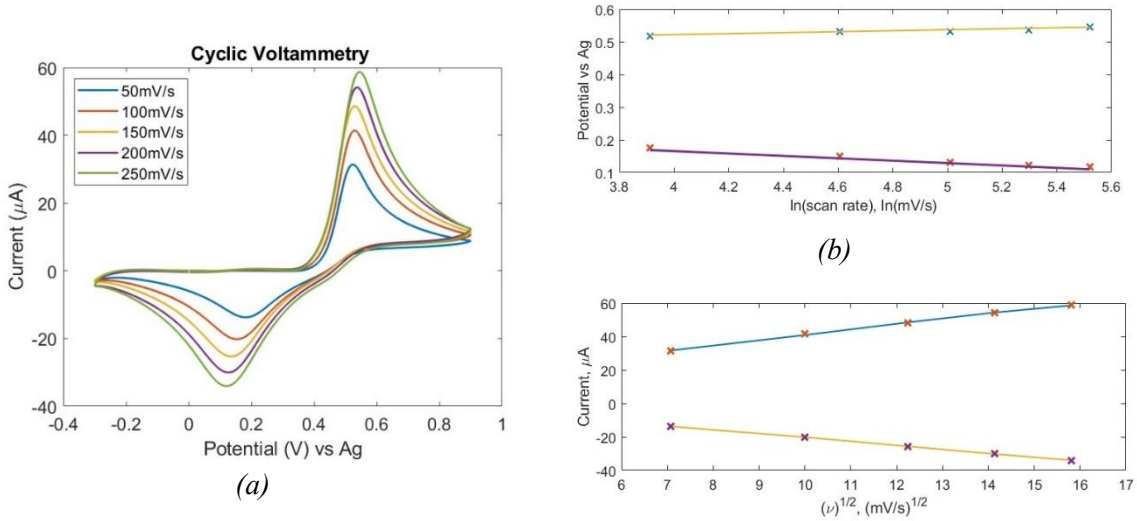

(a)

(b)

(c)

Figure 21 - (a) Cyclic voltammetry for the detection of 1mM of paracetamol in 0.1M PBS with a BP1 electrode, change in the scan rate from 50 mV/s to 250 mV/s, (b) dependence of the positions of the potential peaks respect the logarithm of scan rate, (c) dependence of the current anodic and cathodic peaks respect the square root of the scan rate

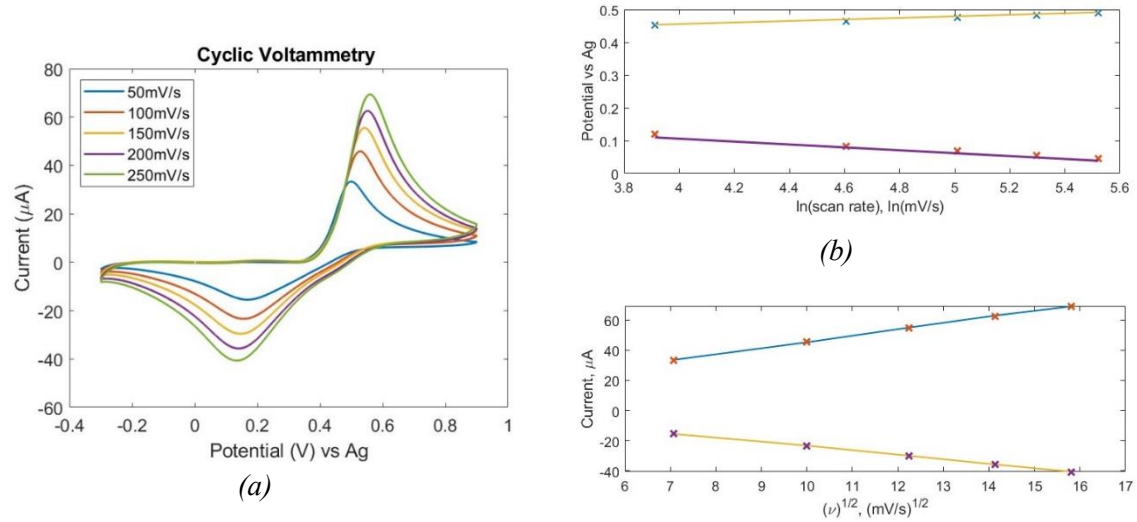

(a)

(b)

(c)

Figure 22 - (a) Cyclic voltammetry for the detection of 1mM of paracetamol in 0.1M PBS with a BP2 electrode, change in the scan rate from 50 mV/s to 250 mV/s, (b) dependence of the positions of the potential peaks respect the logarithm of scan rate, (c) dependence of the current anodic and cathodic peaks respect the square root of the scan rate

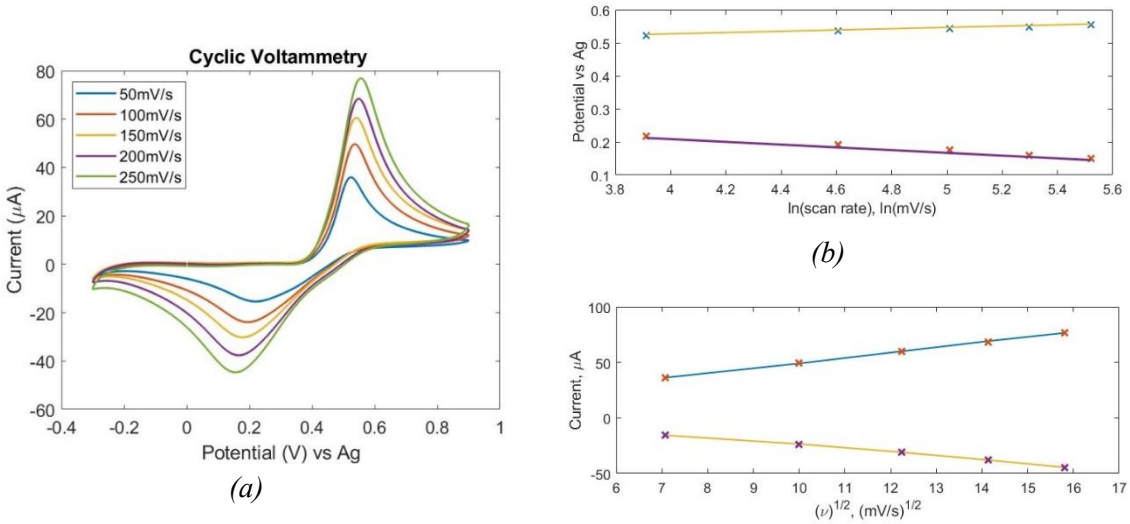

(a)

(b)

(c)

Figure 23 - (a) Cyclic voltammetry for the detection of 1mM of paracetamol in 0.1M PBS with a BP4 electrode, change in the scan rate from 50 mV/s to 250 mV/s, (b) dependence of the positions of the potential peaks respect the logarithm of scan rate, (c) dependence of the current anodic and cathodic peaks respect the square root of the scan rate

ELECTRODE	$I_{pa}(\mu A)$	R^2	$I_{pc}(\mu A)$	R^2
BARE	$2.39\sqrt{v} + 8.96$	0.996	$-2.10\sqrt{v} + 2.90$	0.999
BP0	$3.33\sqrt{v} + 7.95$	0.999	$-2.50\sqrt{v} + 4.22$	0.999
BP1	$3.13\sqrt{v} + 9.65$	0.998	$-2.80\sqrt{v} + 2.30$	0.999
BP2	$4.11\sqrt{v} + 5.21$	0.999	$-2.90\sqrt{v} + 4.49$	0.999
BP4	$4.65\sqrt{v} + 3.05$	0.999	$-2.30\sqrt{v} + 8.80$	0.993

Table 7 – PCM - Linear regression current equation respects the scan rate and regression coefficients of all the studied SPEs

ELECTRODE	ΔE_P (mV)	R^2
BARE	$52.4 \cdot ln(v) + 262.7$	0.993
BP0	$51.3 \cdot ln(v) + 120.2$	0.995
BP1	$56.1 \cdot ln(v) + 118.9$	0.994
BP2	$69.1 \cdot ln(v) + 62.0$	0.998
BP4	$61.8 \cdot ln(v) + 61.5$	0.994

Table 8 – PCM - Linear regression equation of the peak potential respect the logarithm of the scan rate and regression coefficient of all the studied SPEs

4.2.2 Paracetamol - Sensitivity and Detection

All the measured parameters and the kinetic studies performed on the SPEs confirmed that the electrochemical detection of paracetamol is a quasi-reversible mechanism, and the developed sensors have the potential for amperometric detection use. To characterize the performance of the modified SPEs it is necessary to study the behaviour at different analyte concentrations. The scan rate is fixed to 100 mV/s and the four values of analyte in 0.1M of PBS are considered (0.5mM, 1mM, 2mM, 3mM). To characterize the response of the sensor the oxidation peak current is taken as the reference value. The obtained values depend on the concentration of the analyte and the result is the calibration curve in Figure 24.

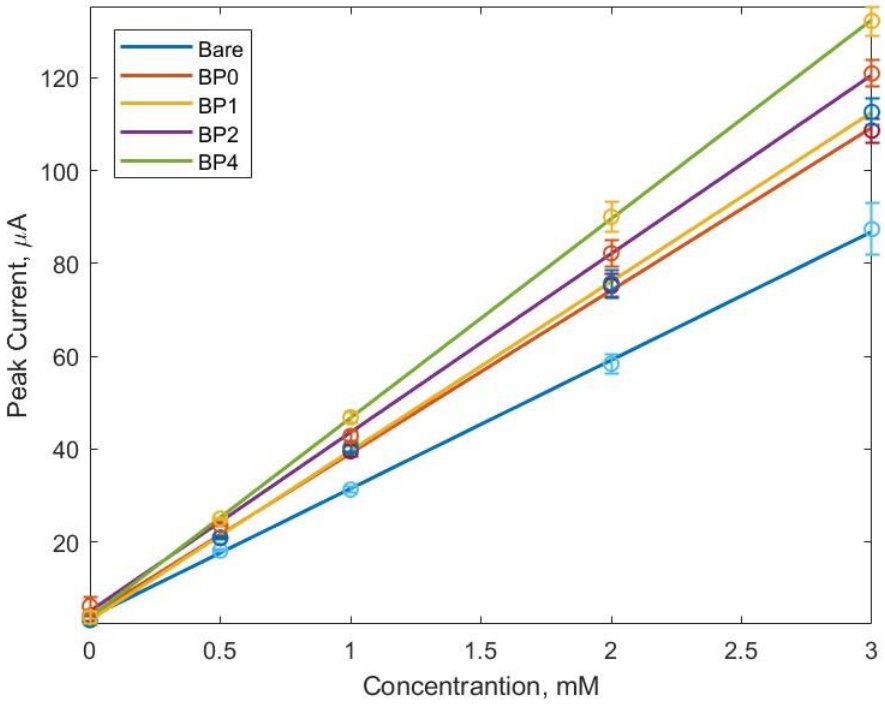

Figure 24 – PCM - Sensitivity curves of different SPEs calculated at different paracetamol concentrations with a scan rate of 100mV/s

It is important to introduce two definitions very useful and widely used in the sensor field. The sensitivity S[μA/mM] is considered as the slope of the plot in Figure 24 and it is related to the change of signal with respect to the variation of the analyte concentration. The Limit of Detection (LOD) is the point at which the analysis is feasible, the minimum amount of signal that is distinguished by noise. Analytically the LOD is calculated as:

$$LOD = \frac{3\,\sigma}{S} \tag{1.26}$$

where σ is the standard deviation of the baseline signal and S is the sensitivity previously obtained. The cyclic voltammograms for the different analyte concentrations are presented in Figure 25 for all the sensors studied and the obtained results are reported in Table 9 and Table 10.

ELECTRODE	$Sensitivity(\mu A/mM)$	$LOD(\mu M)$	RSD
BARE	27.68 ± 0.30	3.28 ± 0.06	1.08%
BP0	35.08 ± 0.44	3.42 ± 0.06	1.25%
BP1	36.46 ± 0.36	2.10 ± 0.09	0.99%
BP2	38.50 ± 0.54	3.48 ± 0.08	1.40%
BP4	42.82 ± 0.48	1.14 ± 0.08	1,12%

Table 9 – PCM - Sensitivity and limit of detection

ELECTRODE	$I_{pa}(\mu A)$	R^2
BARE	$27.68 \cdot c$ + 3.82	0.999
BP0	$35.08 \cdot c$ + 4.03	0.999
BP1	$36.46 \cdot c$ + 3.16	0.999
BP2	$38.50 \cdot c$ + 6.20	0.998
BP4	$42.82 \cdot c$ + 3.84	0.999

Table 10 – PCM - Linear regression current line respects to concentration

The obtained results highlight the electrocatalytic effect of the bismuth compounds. Their deposition on the working electrode increases the sensitivity of the sensor. Also in the sensitivity analysis, the improvement is related to the amount of PEG used in the synthesis process of the microstructures. The value of the sensitivity increases from BP0 to BP4 and it could be related to the presence of more favourable sites for the interaction between the working electrode surface and the analyte, see SEM analysis in Section 3.4.

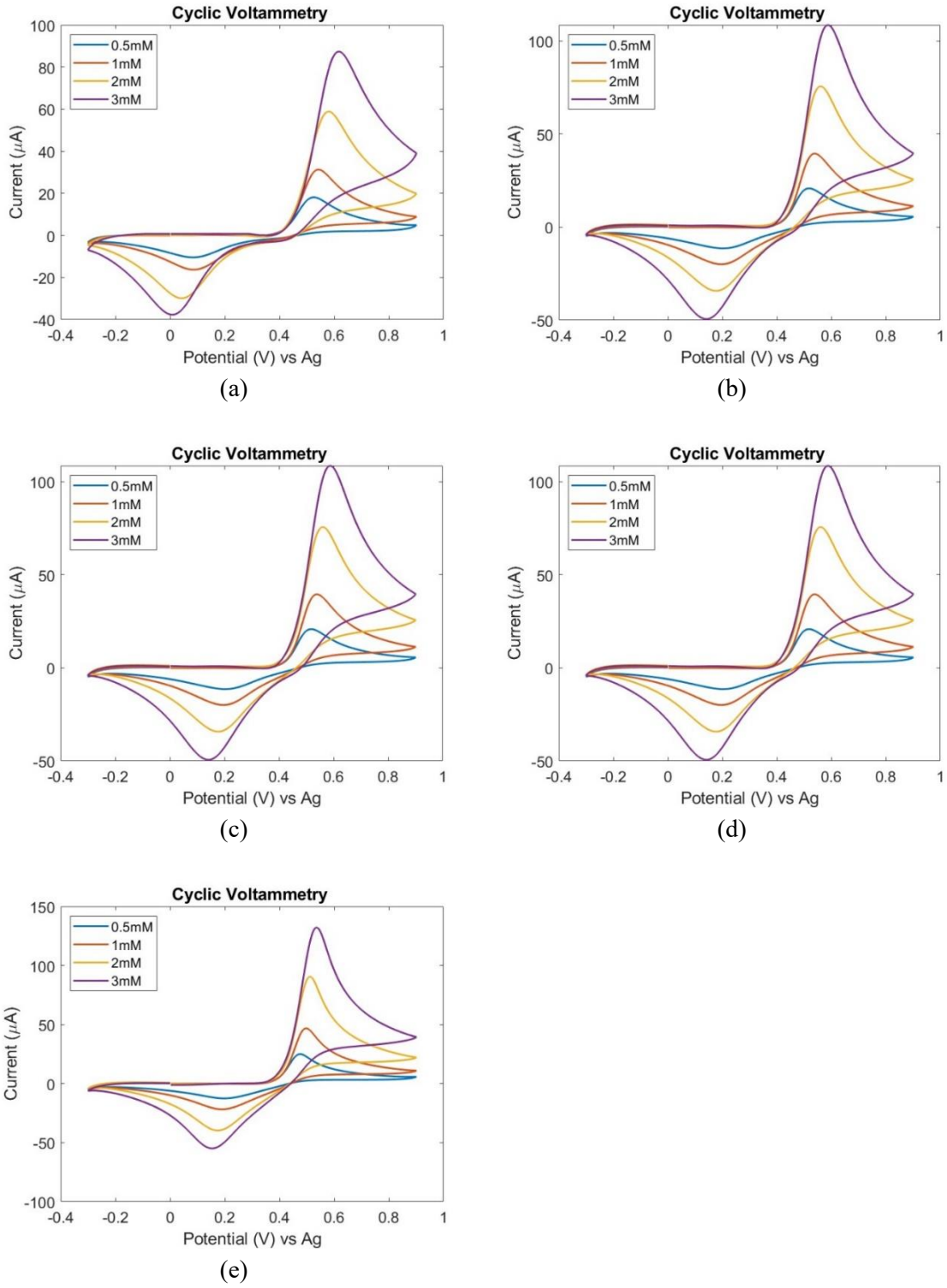

Figure 25 – PCM - Cyclic Voltammograms for different paracetamol concentrations at scan rate of 100 mV/s of the sensor (a) Bare, (b) BP0, (c) BP1, (d) BP2, (e) BP4

4.3 Cyclic Voltammetry – Dopamine

The same procedure of characterization was done for the detection of Dopamine [DA]. Also, in this case five sensors were studied (Bare – BP0 – BP1 – BP2 – BP4) to determine how the bismuth-based materials change the electrodes performance. The theory used for the determination of all the relevant parameters is based always on the Randles-Sevich equation and the Laviron model.

4.3.1 Dopamine – Kinetic Characterization

The electrochemical oxidation of the dopamine is a 2-electron process like the paracetamol. The mechanism is represented in Figure 26 and involves the production of dopaminoquinone [71].

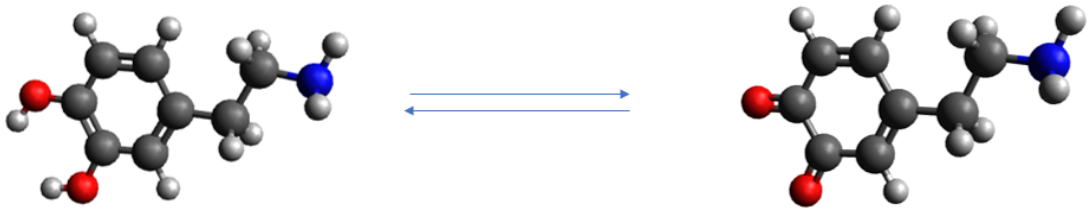

Figure 26 – DA - Mechanism of electrochemical oxidation [Avogadro® optimization]

The first comparison performed is between the electrolytic solution of only 0.1M PBS and the same solution with a concentration of 1mM of dopamine at a scan rate of 100 mV/s. The results are shown in Figure 27, where it is possible to see the presence of the anodic peak and the smaller cathodic one. The electrochemical oxidation of dopamine is a quasi-reversible process, the oxidation peak is greater respect the reduction one because the process is not equally balanced.

The comparison of the sensors performance is highlighted by the detection of a concentration of 1mM of dopamine in 0.1M PBS with a scan rate of 100 mV/s. Figure 28 shows the electrocatalytic effect of the Bismuth in dopamine detection. There is a great difference in the oxidation current peak if the electrode is modified and an interesting difference if the PEG was used in bismuth-based materials synthesis. A strong improvement is also present in the potential position of the peak. ΔE_p is considered a benchmark of how an electrochemical process is favourable and Figure 28 shows that its value is reduced for the modified electrodes.

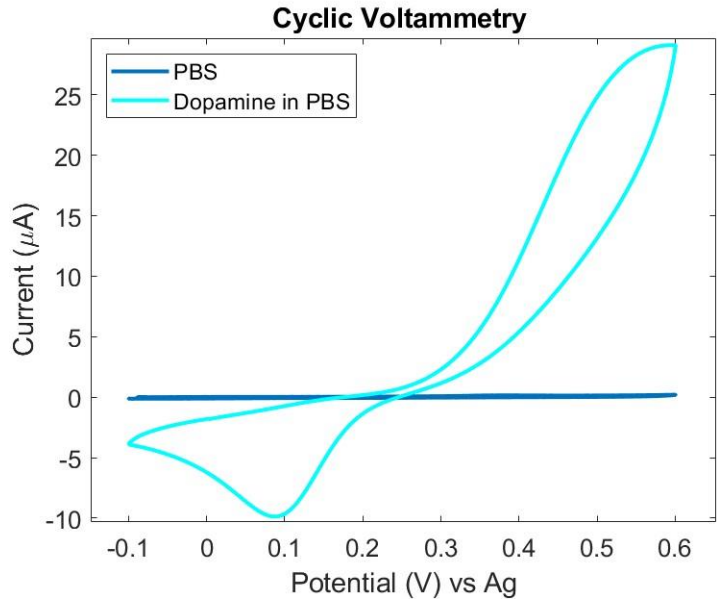

Figure 27 – DA - Cyclic voltammetry with and without dopamine in 0.1M PBS

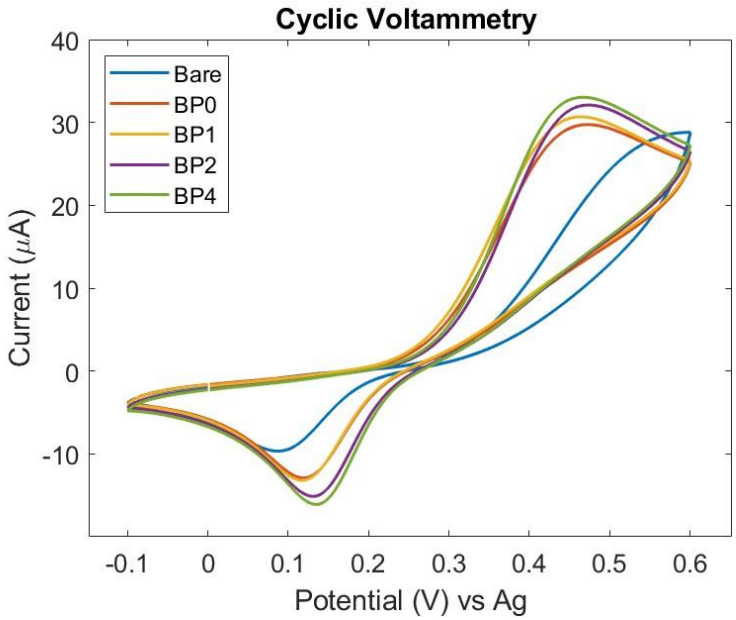

Figure 28 – DA - Comparison between the bare electrode and the modified ones. Concentration of dopamine of 1mM in 0.1M PBS at scan rate of 100mV/s

From the cyclic voltammograms of dopamine, it is possible to notice that its electroactivity is different with respect to paracetamol. In the case of the PCM, the peaks present a marker feature, indicating a simple process of approaching the molecule with the electrode surface through the electrolyte. The electroactivity of dopamine seems more a capacitive process, in the sense that the diffuse layer between the two phases could present charge accumulation related to a particular positioning of the dopamine molecules. This is a hypothesis that could require advanced study to be

validated but it seems a valid standpoint. In any case due to the presence of a capacitive process more evident in the dopamine analysis, particular attention to the search peak is needed in order to compare only the faradaic current related to the process.

ELECTRODE	$I_{pa}(\mu A)$
BARE	9.84 ± 0.52
BP0	14.41 ± 0.77
BP1	17.92 ± 0.89
BP2	18.33 ± 0.65
BP4	19.99 ± 0.79

Table 11 – DA - Anodic peak current of different electrodes.

Table 12 summarizes the kinetic parameters calculated through the Laviron theory presented in Section 1. The charge transfer coefficient α is reduced for the modified electrodes and the kinetic rate constant increases from 3.93 ± 0.40 ms^{-1} for the bare electrode to 24.14 ± 4.63 for the electrode modified with BP4 material.

ELECTRODE	ΔE_P (mV)	α	D(cm^2/s)	Rate constant k (ms^{-1})
BARE	376 ± 14	0.47 ± 0.12	$1.16 \cdot 10^{-7}$	3.93 ± 0.40
BP0	321 ± 11	0.41 ± 0.13	$2.44 \cdot 10^{-7}$	13.27 ± 3.38
BP1	295 ± 15	0.39 ± 0.13	$3.83 \cdot 10^{-7}$	21.92 ± 4.48
BP2	295 ± 22	0.38 ± 0.11	$4.04 \cdot 10^{-7}$	21.07 ± 1.13
BP4	296 ± 24	0.38 ± 0.15	$4.28 \cdot 10^{-7}$	24.14 ± 4.63

Table 12 – DA - Kinetic parameters of different SPEs

In Figure 29 cyclic voltammetry analyses performed on each electrode are presented. The scan rate was varied in the range between 50 mV/s and 300 mV/s with a step of 50 mV/s. The concentration of dopamine is fixed at 1mM and the behaviour of the anodic peak with respect to the scan rate is evaluated.

ELECTRODE	ΔE_P (mV)	R^2
BARE	$22.2 \cdot ln(v) + 267.5$	0.993
BP0	$17.7 \cdot ln(v) + 235.1$	0.993
BP1	$23.5 \cdot ln(v) + 180.3$	0.996
BP2	$34.2 \cdot ln(v) + 127.8$	0.993
BP4	$37.2 \cdot ln(v) + 116.7$	0.998

Table 13 – DA - Linear regression equation of the peak potential respect the logarithm of the scan rate and regression coefficient of all the studied SPEs

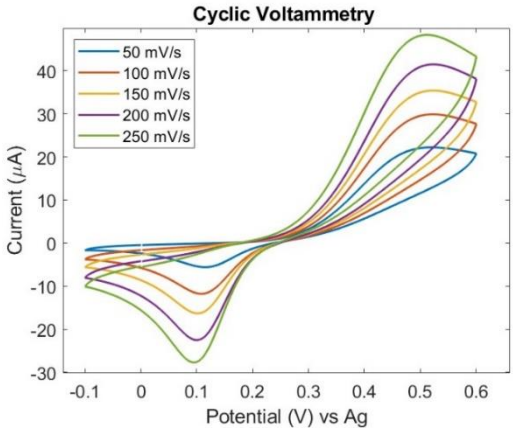

(a)

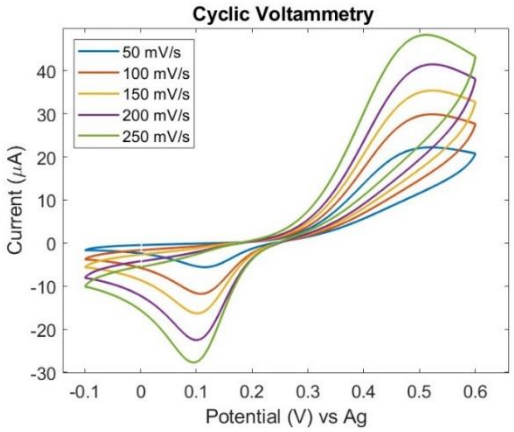

(b)

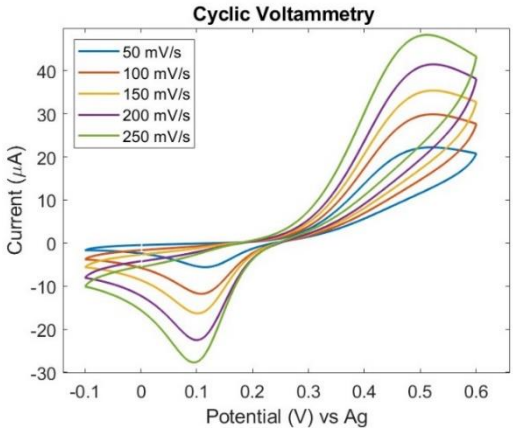

(c)

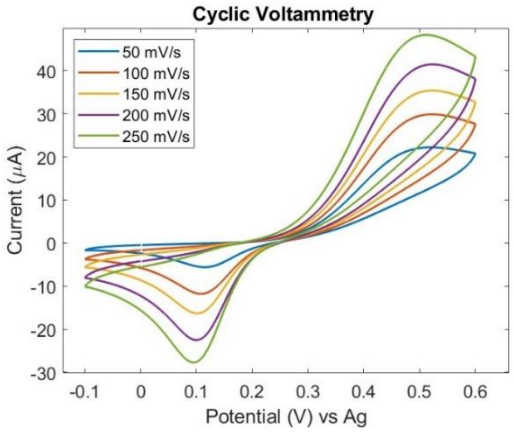

(d)

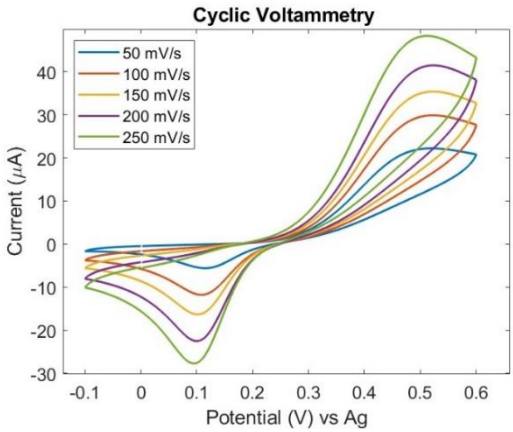

(e)

Figure 29 – Cyclic voltammetry for the detection of 1mM of dopamine in 0.1M PBS, change in the scan rate from 50 mV/s to 250 mV/s for the (a) Bare, (b) BP0, (c) BP1, (d) BP2, (e) BP4

From the behaviour of the peak currents respect the variation of the scan rate, it is possible to evaluate the interaction mechanism of the analyte. In the case of the PCM previously studied, the peak current increases with the square root of the scan rate because it is diffusion-controlled. In the case of the DA it is proven the linearity of the peak with the scan rate in Figure 30, this behaviour demonstrates that the process is adsorption controlled. This result is in agreement with the work of Venton et al. on dopamine electrochemical detection [72].

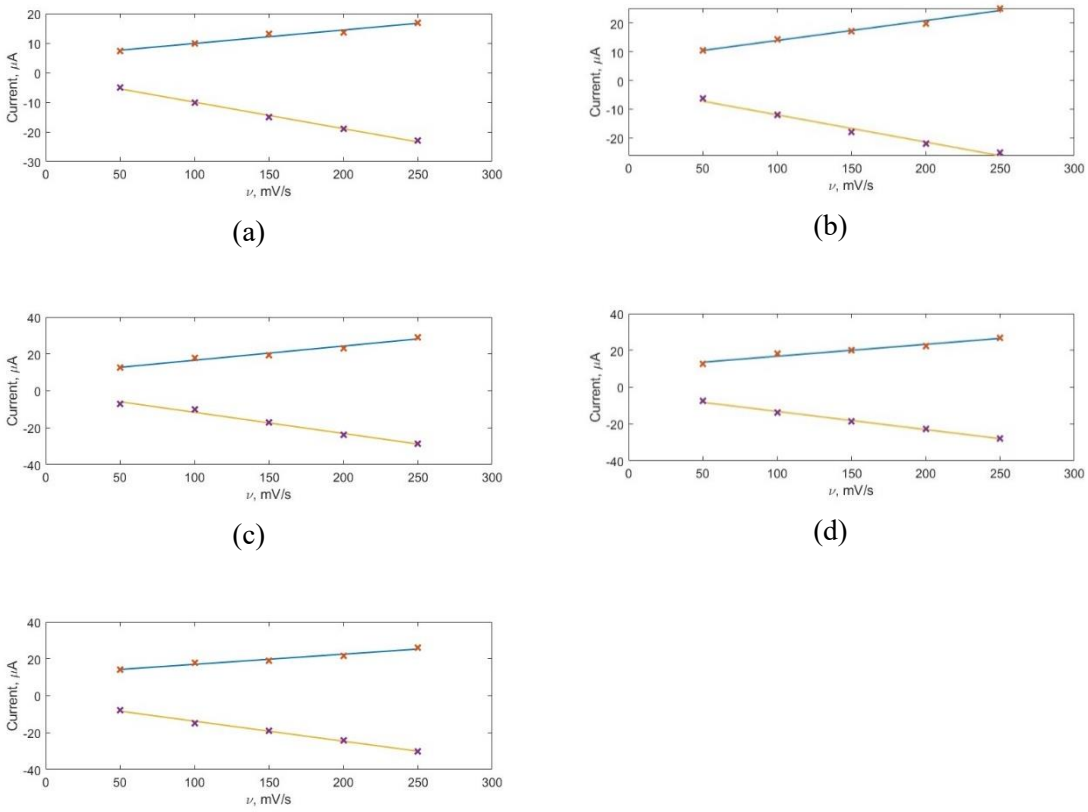

Figure 30 – DA - Dependence of the current anodic and cathodic peaks respect the scan rate for the (a) Bare, (b) BP0, (c) BP1, (d) BP2, (e) BP4

ELECTRODE	$I_{pa}(\mu A)$	R^2	$I_{pc}(\mu A)$	R^2
BARE	$(4.5* 10^{-2})$ υ + 5.3	0.983	$(-8.8* 10^{-2})$ υ – 1.2	0.997
BP0	$(6.9* 10^{-2})$ υ + 7.0	0.982	$(-9.6 * 10^{-2})$ υ – 2.2	0.988
BP1	$(7.7* 10^{-2})$ υ + 8.9	0.967	$(-11.4* 10^{-2})$ υ – 0.2	0.987
BP2	$(6.5* 10^{-2})$ υ + 10.4	0.963	$(-9.9* 10^{-2})$ υ – 3.3	0.995
BP4	$(5.3* 10^{-2})$ υ + 12.0	0.960	$(-10.8* 10^{-2})$ υ – 2.9	0.993

Table 14 – DA - Linear regression current equation respects the scan rate and regression coefficients of all the studied SPEs

4.3.2 Dopamine – Sensitivity and Detection

The dopamine sensors need to be characterized from the sensitivity point of view. To construct the calibration curves of each sensor, cyclic voltammetry analyses for five dopamine concentrations (0.1mM, 0.5mM, 1mM, 2.5mM, 5mM) were performed. The scan rate was fixed at 100 mV/s for each measurement and the height of the oxidation peak was taken. The value of the peak obtained is represented with respect to the dopamine concentration in Figure 31, where the calibration curves were obtained.

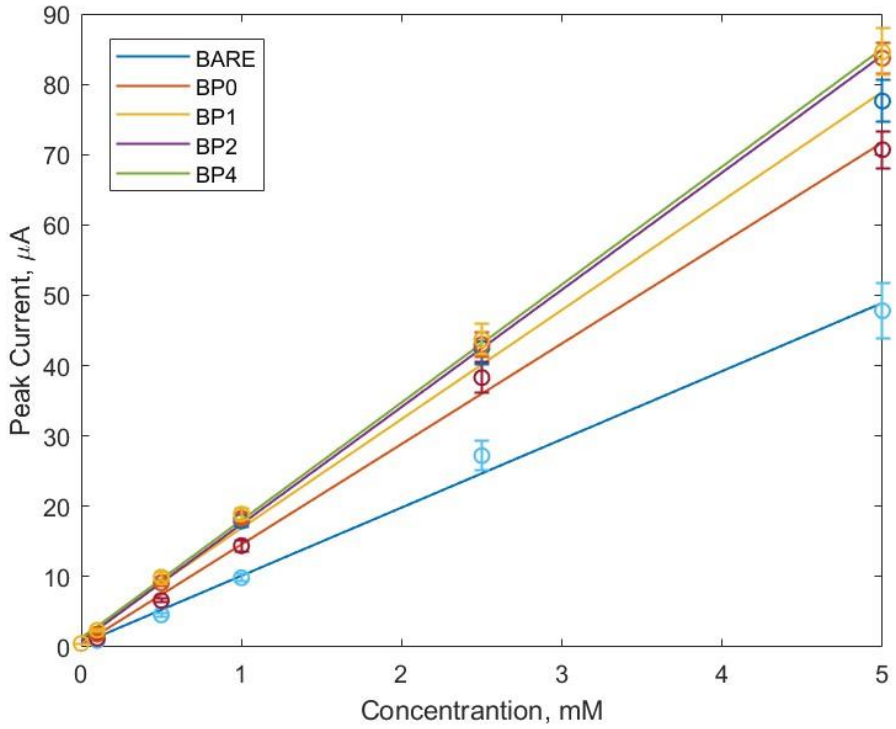

Figure 31 – DA - Sensitivity curves of different SPEs calculated at different dopamine concentrations with a scan rate of 100mV/s

For each sensor, the sensitivity is calculated as the slope of the respective calibration curve and the limit of detection is calculated by considering the formula (1.26). The results of the calculations are listed in Table 15.

Bare electrode has a sensitivity of 9.71 ± 1.23 $\mu A/mM$ with a LOD of 8.47 ± 2.64 μM. All the modified electrodes present a greatly increased sensitivity. Among them, the higher value is related to the electrode modified with BP4 material that has a value of 16.67 ± 1.31 $\mu A/mM$, quite double with respect to the bare electrode one.

ELECTRODE	$Sensitivity(\mu A/mM)$	$LOD(\mu M)$	RSD
BARE	9.71 ± 1.23	8.47 ± 2.64	12.7%
BP0	14.43 ± 0.56	9.89 ± 1.11	3.9%
BP1	15.41 ± 0.59	5.33 ± 0.85	3.8%
BP2	16.62 ± 0.83	2.18 ± 0.63	4.9%
BP4	16.67 ± 1.31	2.38 ± 1.21	7.8%

Table 15 – DA - Sensitivity and limit of detection

According to the theory, the value of the LOD should decrease for highly sensitive sensors, but it does not happen in the case of BP0 which presents a LOD of 9.89 ± 1.11 μM. It is related to the fact that the value of the LOD is quite delicate because it depends on the standard deviation of the blank measurement, which is an analytical parameter. Instead, the electrodes modified with BP1, BP2, and BP4 seem to follow the theory prediction with lower values with respect to the bare one.

ELECTRODE	$I_{pa}(\mu A)$	R^2
BARE	$9.71 \cdot c$ + 0.41	0.994
BP0	$14.43 \cdot c$ + 0.58	0.995
BP1	$15.41 \cdot c$ + 1.74	0.997
BP2	$16.62 \cdot c$ + 0.95	0.999
BP4	$16.67 \cdot c$ + 1.56	0.999

Table 16 – DA - Linear regression current line respects to concentration

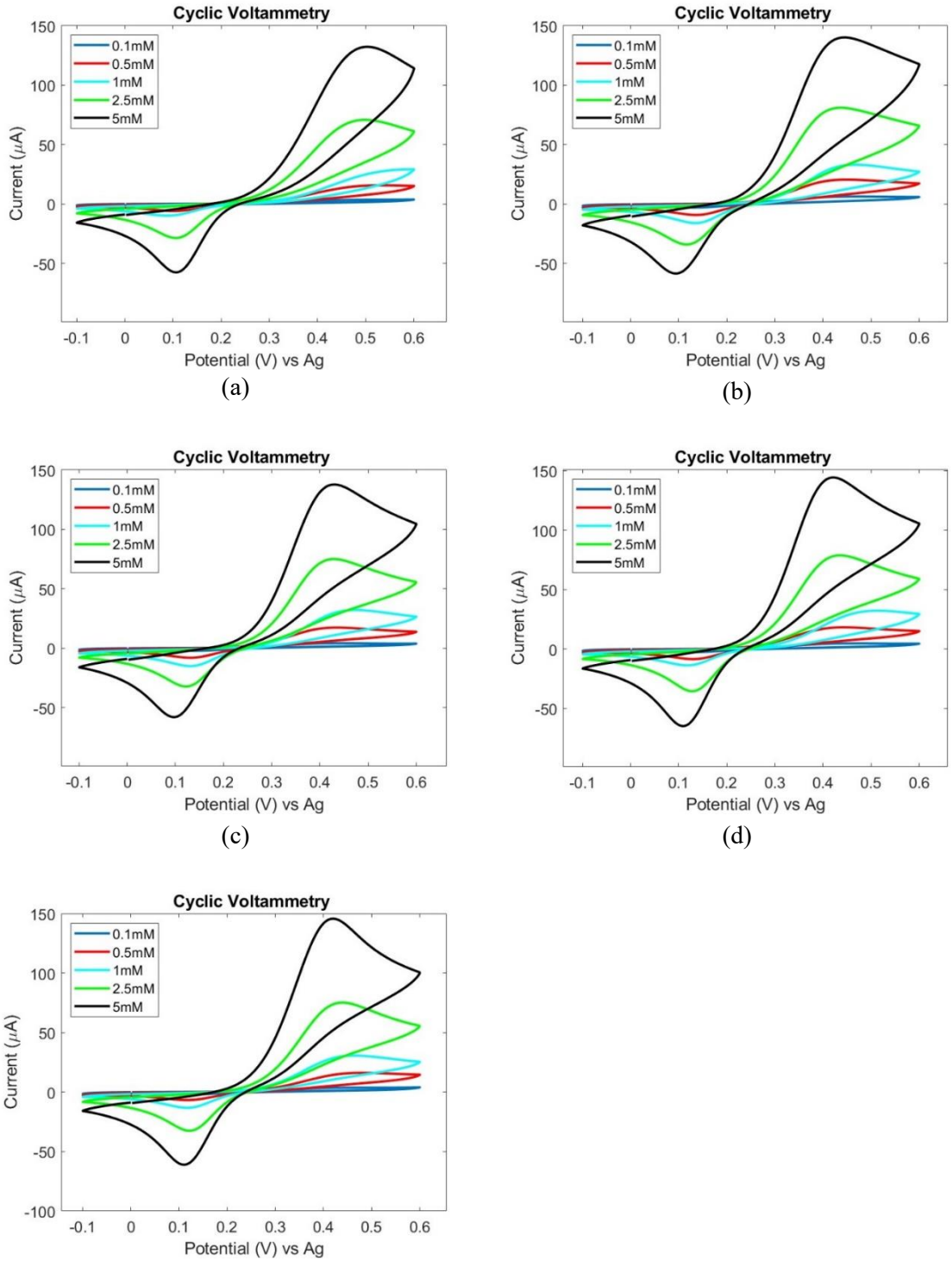

Figure 32 – DA - Cyclic Voltammograms for different dopamine concentrations at scan rate of 100 mV/s of the sensor (a) Bare, (b) BP0, (c) BP1, (d) BP2, (e) BP4

4.4 Cyclic Voltammetry - Uric Acid

4.4.1 Uric Acid – Kinetic Characterization

Electrochemical detection is a technique that could involve also irreversible processes. It is the case of Uric Acid (UA) detection, where the application of a specific potential induces the irreversible oxidation of the molecule.

Figure 33 – UA - Mechanism of electrochemical oxidation [Avogadro® optimization]

The electrochemical oxidation of the uric acid is a multistep process that ends with the rupture of the aromatic ring. It is a 2-electron process that initially produces a diamine molecule. Considering the instability of the diamine, it hydrates two times passing through the form of imine-alcohol and uric acid-4,5-diol. The last step is the decomposition of the molecule in neutral pH which produces an allantoin molecule and a CO_2 molecule [73] [74].

The formation of the new compound does not allow the restoration of the molecule that remains unchanged, and it is impossible to induce the reduction. The cyclic voltammetry obtained with the bare electrode is shown in Figure 34 where only the anodic peak is present.

Figure 35 shows the comparison between the cyclic voltammetry of the bare electrode and the ones obtained with the modified electrodes (BP0 and BP1). As in the case of the previous analytes, the bismuth compounds present good electrocatalytic properties increasing the oxidation peak current (see Table 17).

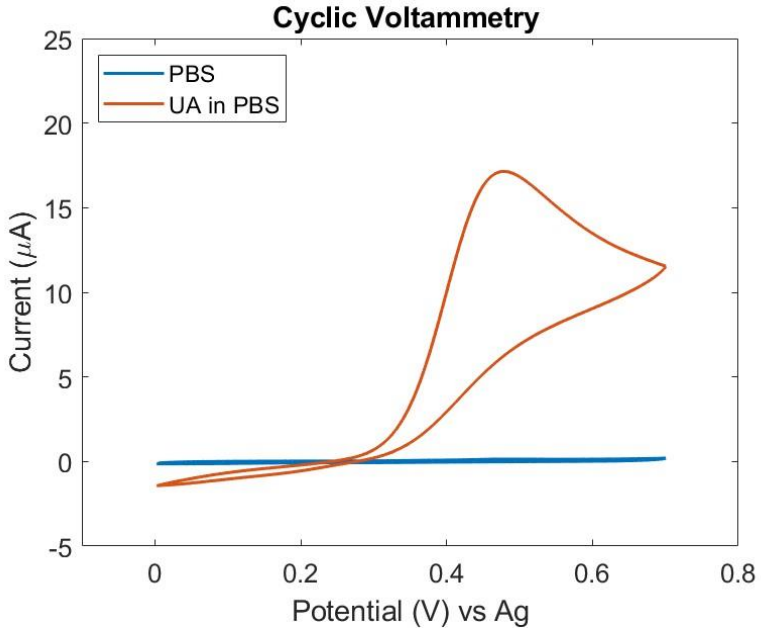

Figure 34 – UA - Cyclic Voltammetry with and without 1mM uric acid in 0.1M PBS at scan rate of 100mV/s

ELECTRODE	$I_{pa}(\mu A)$
BARE	11.11 ± 0.35
BP0	13.31 ± 0.45
BP1	13.42 ± 0.46

Table 17 – UA - Oxidation Peak Current

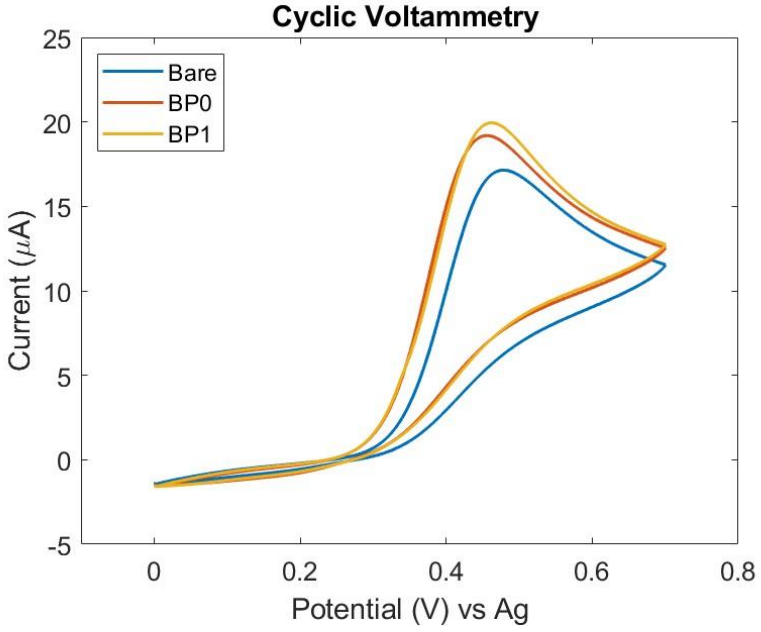

Figure 35 – UA - Comparison between the bare electrode and the modified ones. Concentration of uric acid of 1mM in 0.1M PBS at scan rate of 100mV/s

4.4.2 Uric Acid - Sensitivity and Detection

The performances of the SPEs as sensors are studied by changing the analyte concentration to construct the calibration plots (see Figure 36). From the plots, it is possible to notice the effect of the bismuth compound action. The value of the sensitivity, resumed in Table 18, passes from a value of $7.14 \pm 0.23\ \mu A/mM$ for the bare electrode to $9.37 \pm 0.29\ \mu A/mM$ for the modified BP0.

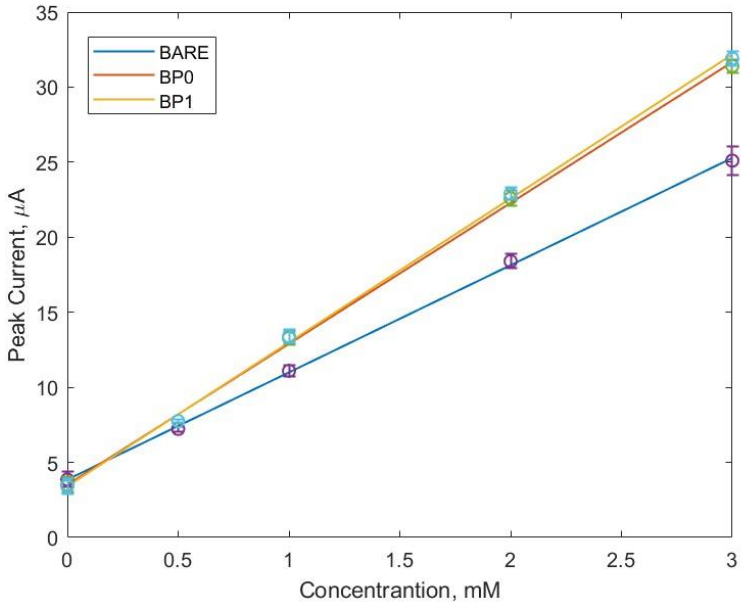

Figure 36 – UA - Sensitivity curves of different SPEs calculated at different uric acid concentrations with a scan rate of 100mV/s

ELECTRODE	$Sensitivity(\mu A/mM)$	$LOD(\mu M)$	RSD
BARE	7.14 ± 0.23	2.53 ± 0.09	3.2%
BP0	9.37 ± 0.29	3.31 ± 0.10	3.1%
BP1	9.59 ± 0.14	3.21 ± 0.09	1.5%

Table 18 – UA - Sensitivity and limit of detection

Particular attention in this analysis was given to the washing electrode procedure. Considering that the electrochemical oxidation of the uric acid is an irreversible process that produces several compounds that remain in the solution. It is possible to mention the CO_2 molecules in the last step and protons in the early stage of the process. After a measurement, the solution is acidified in the region close to the electrode and some compounds could remain attached to the surface. To guarantee a good reproducibility of the conditions the electrode was washed 3 times with DI water and between two measurements a cyclic voltammetry of blank solution was performed.

ELECTRODE	$I_{pa}(\mu A)$	R^2
BARE	$7.14 \cdot c + 3.86$	0.999
BP0	$9.37 \cdot c + 3.52$	0.998
BP1	$9.59 \cdot c + 3.41$	0.998

Table 19 – UA - Linear regression current line respect to concentration

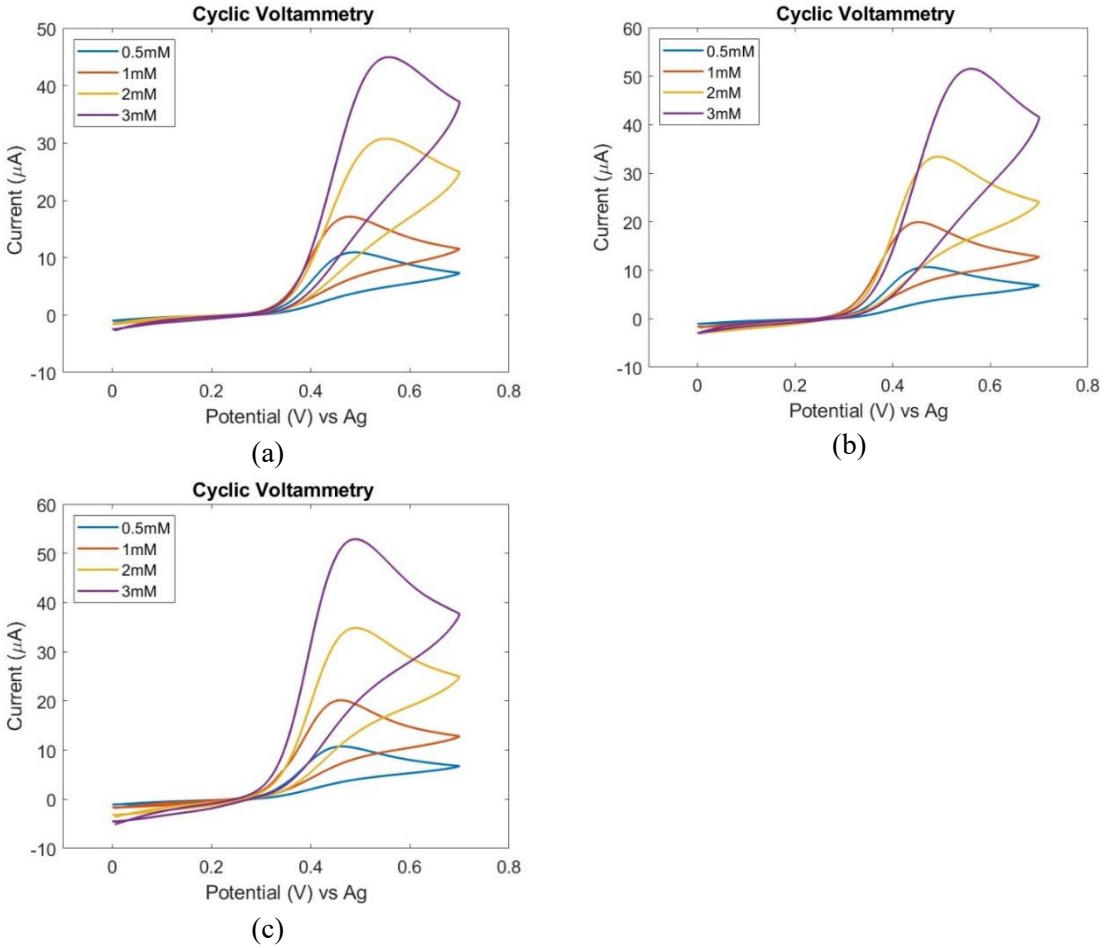

Figure 37 – Cyclic Voltammograms for different uric acid concentrations at scan rate of 100 mV/s of the sensor (a) Bare, (b) BP0, (c) BP1

5 Conclusions

This study makes evidence of the electroactivity of several analytes as paracetamol, dopamine, and uric acid. The electrochemical technique employed was Cyclic voltammetry which allows the study of the interaction between the molecules and the electrode surface. A screen-printed electrode developed by DropSens was employed and the study of the analyte was made in phosphate buffer solution, a neutral pH electrolyte. It was definitively proven the diffusion-limited effect of paracetamol, the adsorption-controlled effect of dopamine and the irreversible process that occurs in the electrochemical oxidation of uric acid. Also, the electrocatalytic effect of bismuth microstructures was tested. Bismuth materials were synthesized with the use of a tip-sonicator with different concentrations of polyethylene glycol used as a surfactant. Four bismuth oxynitrates were prepared: BP0, BP1, BP2, and BP4 where the number in the name indicates the PEG/Bismuth ratio employed. SPEs were modified with the previous materials to study the effect of the use of PEG on the electrochemical behaviour of the new sensors for the previous analytes. The development of new SPEs has been done by modifying the working electrode with drop-casting technique of water-based bismuth solutions. The first study of the resistance of the electrodes was done by Electrochemical Impedance Spectroscopy. The measurement confirms the reduction of the interface resistance for the bismuth-modified electrode, which goes from 569.9 Ω for the bare electrode to a range of [209.7 – 325.7] Ω for the modified ones.

The kinetic characterization of the sensors was studied by performing cyclic voltammetry at different scan rates in the range of 50 mV/s and 250 mV/s of 1mM of the analyte. According to the Laviron theory, kinetic rate constant k and electron transfer coefficient α were calculated. It was proven that the use of the PEG during the material synthesis allows the development of improved electrocatalytic structures. In the paracetamol analysis, the kinetic rate constant passes from 0.69 ± 0.29 ms^{-1} for the bare electrode, to 1.60 ± 0.40 ms^{-1} for the BP0, and 5.72 ± 0.67 ms^{-1} for the BP4. In the dopamine analysis, similar results were obtained: the rate constant increased from 3.93 ± 0.40 ms^{-1} for the bare electrode to 24.14 ± 4.63 ms^{-1} for the BP4 modified.

Cyclic voltammetry was performed also to characterize the sensors in terms of sensitivity and limit of detection. Several measurements were done by changing the concentration of the analyte in the solution and the variation of the anodic peak current was investigated. It was observed a linear response for all electrodes. In the case of paracetamol, the mean sensitivity of the bare electrode was 27.68 ± 0.30 μA/mM with a LOD of 3.28 ± 0.06 μM. In terms of sensitivity, all the modified electrodes presented increased values, where the highest value (42.82 ± 0.48 μA/mM) was the one of the BP4 modified electrode. In the dopamine analysis, the sensitivity passes from a value of 9.71 ± 1.23 μA/mM for the bare electrode to 14.43 ± 0.56 μA/mM for the BP0 and 16.67 ± 1.31 μA/mM for the BP4.

Also in the uric acid analysis, the electrocatalytic effect of the bismuth was proven. The mean sensitivity for the bare electrode in the study of uric acid was 7.14 ± 0.23 μA/mM. This value increases to 9.37 ± 0.29 μA/mM in the case of BP0 performance and 9.59 ± 0.14 μA/mM for BP1. These results confirm the electroactivities of the analytes studied and the electrocatalytic behaviour of the oxynitrates bismuth structures. This opens the way to a deeper understanding of the synthesis process of bismuth composites and its potential in the development of new sensors.

Bibliography

[1] V. Naresh e N. Lee, «A Review on Biosensors and Recent Development of Nanostructured Materials-Enabled Biosensors», *Sensors*, vol. 21, fasc. 4, Art. fasc. 4, gen. 2021, doi: 10.3390/s21041109.

[2] S. J. Sadeghi, «Amperometric Biosensors», in *Encyclopedia of Biophysics*, G. C. K. Roberts, A c. di, Berlin, Heidelberg: Springer, 2013, pp. 61–67. doi: 10.1007/978-3-642-16712-6_713.

[3] B. Mattiasson, C. Borrebaeck, B. Sanfridson, e K. Mosbach, «Thermometric enzyme linked immunosorbent assay: TELISA», *Biochim. Biophys. Acta*, vol. 483, fasc. 2, pp. 221–227, ago. 1977, doi: 10.1016/0005-2744(77)90050-x.

[4] I. Incaviglia, S. Herzog, G. Fläschner, N. Strohmeyer, E. Tosoratti, e D. J. Müller, «Tailoring the Sensitivity of Microcantilevers To Monitor the Mass of Single Adherent Living Cells», *Nano Lett.*, vol. 23, fasc. 2, pp. 588–596, gen. 2023, doi: 10.1021/acs.nanolett.2c04198.

[5] A. Vijayalakshmi *et al.*, «Enzyme field effect transistor (ENFET) for estimation of triglycerides using magnetic nanoparticles», *Biosens. Bioelectron.*, vol. 23, fasc. 11, pp. 1708–1714, giu. 2008, doi: 10.1016/j.bios.2008.02.003.

[6] G. P. Anderson e C. R. Taitt, «Chapter 2 - EVANESCENT WAVE FIBER OPTIC BIOSENSORS», in *Optical Biosensors (Second Edition)*, F. S. Ligler e C. R. Taitt, A c. di, Amsterdam: Elsevier, 2008, pp. 83–138. doi: 10.1016/B978-044453125-4.50004-8.

[7] «Amperometric - an overview | ScienceDirect Topics». https://www.sciencedirect.com/topics/chemistry/amperometric .

[8] H.-M. Tan, S.-P. Cheong, e T.-C. Tan, «An amperometric benzene sensor using whole cell Pseudomonas putida ML2», *Biosens. Bioelectron.*, vol. 9, fasc. 1, pp. 1–8, gen. 1994, doi: 10.1016/0956-5663(94)80008-1.

[9] K. Kalcher, «A new method for the voltammetric determination of nitrite», *Talanta*, vol. 33, fasc. 6, pp. 489–494, giu. 1986, doi: 10.1016/0039-9140(86)80260-0.

[10] J. Wang e M. Bonakdar, «Preconcentration and voltammetric measurement of mercury with a crown-ether modified carbon-paste electrode», *Talanta*, vol. 35, fasc. 4, pp. 277–280, apr. 1988, doi: 10.1016/0039-9140(88)80085-7.

[11] W. Simon, E. Pretsch, W. E. Morf, D. Ammann, U. Oesch, e O. Dinten, «Design and application of neutral carrier-based ion-selective electrodes. Plenary lecture», *Analyst*, vol. 109, fasc. 3, pp. 207–209, 1984, doi: 10.1039/AN9840900207.

[12] «Application of Electrochemical Biosensors in Clinical Diagnosis», doi: 10.1002/jcla.20500.

[13] A. C. R. GRAYSON *et al.*, «A BioMEMS review: MEMS technology for physiologically integrated devices», *Proc. IEEE*, vol. 92, fasc. 1, pp. 6–21, gen. 2004, doi: 10.1109/JPROC.2003.820534.

[14] «Lab-On-Chip Devices: Materials Considerations». https://www.meddeviceonline.com/doc/lab-on-chip-devices-materials-considerations-0001.

[15] E. Chiam, L. Weinberg, e R. Bellomo, «Paracetamol: a review with specific focus on the haemodynamic effects of intravenous administration», *Heart Lung Vessels*, vol. 7, fasc. 2, pp. 121–132, 2015.

[16] R. T. Stravitz e W. M. Lee, «Acute liver failure», *The Lancet*, vol. 394, fasc. 10201, pp. 869–881, set. 2019, doi: 10.1016/S0140-6736(19)31894-X.

[17] B. D. Clayton e M. Willihnganz, *Basic Pharmacology for Nurses16: Basic Pharmacology for Nurses*. Elsevier Health Sciences, 2013.

[18] D. Easwaramoorthy, Y.-C. Yu, e H.-J. Huang, «Chemiluminescence detection of paracetamol by a luminol-permanganate based reaction», *Anal. Chim. Acta*, vol. 439, fasc. 1, pp. 95–100, lug. 2001, doi: 10.1016/S0003-2670(01)00968-0.

[19] T. Madrakian, A. Afkhami, e M. Mohammadnejad, «Second-order advantage applied to simultaneous spectrofluorimetric determination of paracetamol and mefenamic acid in urine samples», *Anal. Chim. Acta*, vol. 645, fasc. 1, pp. 25–29, lug. 2009, doi: 10.1016/j.aca.2009.05.002.

[20] «Second Derivative Spectrophotometric Determination of p-Aminophenol in the Presence of Paracetamol: Analytical Letters: Vol 24, No 1». https://www.tandfonline.com/doi/abs/10.1080/00032719108052889.

[21] X. ShangGuan, H. Zhang, e J. Zheng, «Electrochemical behavior and differential pulse voltammetric determination of paracetamol at a carbon ionic liquid electrode», *Anal. Bioanal. Chem.*, vol. 391, fasc. 3, pp. 1049–1055, giu. 2008, doi: 10.1007/s00216-008-2096-7.

[22] F. Zamarchi e I. C. Vieira, «Determination of paracetamol using a sensor based on green synthesis of silver nanoparticles in plant extract», *J. Pharm. Biomed. Anal.*, vol. 196, p. 113912, mar. 2021, doi: 10.1016/j.jpba.2021.113912.

[23] K. Alanazi *et al.*, «Disposable paracetamol sensor based on electroactive molecularly imprinted polymer nanoparticles for plasma monitoring», *Sens. Actuators B Chem.*, vol. 329, p. 129128, feb. 2021, doi: 10.1016/j.snb.2020.129128.

[24] X.-Q. Cai, K. Zhu, B.-T. Liu, Q.-Y. Zhang, Y.-H. Luo, e D.-E. Zhang, «γ-Fe2O3/CNTs Composites for Electrochemical Detection of Paracetamol: Synthesis, Phase Transition and Enhanced Properties», *J. Electrochem. Soc.*, vol. 168, fasc. 5, p. 057511, mag. 2021, doi: 10.1149/1945-7111/abfe78.

[25] J. Meiser, D. Weindl, e K. Hiller, «Complexity of dopamine metabolism», *Cell Commun. Signal. CCS*, vol. 11, fasc. 1, p. 34, mag. 2013, doi: 10.1186/1478-811X-11-34.

[26] H. Juárez Olguín, D. Calderón Guzmán, E. Hernández García, e G. Barragán Mejía, «The Role of Dopamine and Its Dysfunction as a Consequence of Oxidative Stress», *Oxid. Med. Cell. Longev.*, vol. 2016, p. 9730467, 2016, doi: 10.1155/2016/9730467.

[27] E. Siegl, B. Lassen, e S. Saxer, «[Incontinence--a common issue for people with Parkinson's disease. A systematic literature review]», *Pflege Z.*, vol. 66, fasc. 9, pp. 540–544, set. 2013.

[28] D. J. Surmeier, J. N. Guzman, J. Sanchez-Padilla, e P. T. Schumacker, «The role of calcium and mitochondrial oxidant stress in the loss of substantia nigra pars compacta dopaminergic neurons in Parkinson's disease», *Neuroscience*, vol. 198, pp. 221–231, dic. 2011, doi: 10.1016/j.neuroscience.2011.08.045.

[29] M. J. Armstrong e M. S. Okun, «Diagnosis and Treatment of Parkinson Disease: A Review», *JAMA*, vol. 323, fasc. 6, pp. 548–560, feb. 2020, doi: 10.1001/jama.2019.22360.

[30] M. Nichkova, P. M. Wynveen, D. T. Marc, H. Huisman, e G. H. Kellermann, «Validation of an ELISA for urinary dopamine: applications in monitoring treatment of dopamine-related disorders», *J. Neurochem.*, vol. 125, fasc. 5, pp. 724–735, 2013, doi: 10.1111/jnc.12248.

[31] P. S. Rao, N. Rujikarn, J. M. Luber, e D. H. Tyras, «A specific sensitive HPLC method for determination of plasma dopamine», *Chromatographia*, vol. 28, fasc. 5, pp. 307–310, set. 1989, doi: 10.1007/BF02260781.

[32] N. O. A. Al-Salahi, E. Y. Hashem, e D. A. Abdel-Kader, «Spectrophotometric Methods for Determination of Dopamine Hydrochloride in Bulk and in Injectable Forms», *Spectrochim. Acta. A. Mol. Biomol. Spectrosc.*, vol. 278, p. 121278, ott. 2022, doi: 10.1016/j.saa.2022.121278.

[33] S. M. Siddeeg, «Electrochemical detection of neurotransmitter dopamine: a review», *Int. J. Electrochem. Sci.*, vol. 15, fasc. 1, pp. 599–612, gen. 2020, doi: 10.20964/2020.01.61.

[34] R. El Ridi e H. Tallima, «Physiological functions and pathogenic potential of uric acid: A review», *J. Adv. Res.*, vol. 8, fasc. 5, pp. 487–493, set. 2017, doi: 10.1016/j.jare.2017.03.003.

[35] M. Jin *et al.*, «Uric Acid, Hyperuricemia and Vascular Diseases», *Front. Biosci. J. Virtual Libr.*, vol. 17, pp. 656–669, gen. 2012.

[36] M. H. Pillinger e B. F. Mandell, «Therapeutic approaches in the treatment of gout», *Semin. Arthritis Rheum.*, vol. 50, fasc. 3, Supplement, pp. S24–S30, giu. 2020, doi: 10.1016/j.semarthrit.2020.04.010.

[37] Q. Wang, X. Wen, e J. Kong, «Recent Progress on Uric Acid Detection: A Review», *Crit. Rev. Anal. Chem.*, vol. 50, fasc. 4, pp. 359–375, lug. 2020, doi: 10.1080/10408347.2019.1637711.

[38] «Electrochemical biosensing of uric acid: A review», *Microchem. J.*, vol. 182, p. 107945, nov. 2022, doi: 10.1016/j.microc.2022.107945.

[39] H. Bi *et al.*, «Carbon-nanotube-modified glassy carbon electrode for simultaneous determination of dopamine, ascorbic acid and uric acid: The effect of functional groups», *Sens. Actuators B Chem.*, vol. 171–172, pp. 1132–1140, ago. 2012, doi: 10.1016/j.snb.2012.06.044.

[40] M. Li, W. Guo, H. Li, W. Dai, e B. Yang, «Electrochemical biosensor based on one-dimensional MgO nanostructures for the simultaneous determination of ascorbic acid, dopamine, and uric acid», *Sens. Actuators B Chem.*, vol. 204, pp. 629–636, dic. 2014, doi: 10.1016/j.snb.2014.08.022.

[41] L. Fu, Y. Zheng, A. Wang, W. Cai, B. Deng, e Z. Zhang, «An Electrochemical Sensor Based on Reduced Graphene Oxide and ZnO Nanorods-Modified Glassy Carbon Electrode for Uric Acid Detection», *Arab. J. Sci. Eng.*, vol. 41, fasc. 1, pp. 135–141, gen. 2016, doi: 10.1007/s13369-015-1621-1.

[42] M. Bartoli, P. Jagdale, e A. Tagliaferro, «A Short Review on Biomedical Applications of Nanostructured Bismuth Oxide and Related Nanomaterials», *Mater. Basel Switz.*, vol. 13, fasc. 22, p. 5234, nov. 2020, doi: 10.3390/ma13225234.

[43] H. Kodama, «Synthesis of a New Compound, Bi5O7NO3, by Thermal Decomposition», *J. Solid State Chem.*, vol. 112, fasc. 1, pp. 27–30, set. 1994, doi: 10.1006/jssc.1994.1259.

[44] L. Ma, J. Wu, S. Wang, H. Yang, D. Liang, e Z. Lu, «Synergistic antibacterial effect of Bi2S3 nanospheres combined with ineffective antibiotic gentamicin against methicillin-resistant Staphylococcus aureus», *J. Inorg. Biochem.*, vol. 168, pp. 38–45, mar. 2017, doi: 10.1016/j.jinorgbio.2016.12.005.

[45] M. Varposhti, A. Abdi Ali, e P. Mohammadi, «Synergistic Effects of Bismuth Thiols and Various Antibiotics Against Pseudomonas aeruginosa Biofilm», *Jundishapur J. Microbiol.*, vol. 7, fasc. 3, p. e9142, mar. 2014, doi: 10.5812/jjm.9142.

[46] D. Ws. Bierer, «Bismuth Subsalicylate: History, Chemistry, and Safety», *Rev. Infect. Dis.*, vol. 12, fasc. Supplement_1, pp. S3–S8, gen. 1990, doi: 10.1093/clinids/12.Supplement_1.S3.

[47] M. Sayed *et al.*, «Bismuth-Doped Nano Zerovalent Iron: A Novel Catalyst for Chloramphenicol Degradation and Hydrogen Production», *ACS Omega*, vol. 5, fasc. 47, pp. 30610–30624, dic. 2020, doi: 10.1021/acsomega.0c04574.

[48] T. Gao *et al.*, «Morphology effects of bismuth catalysts on electroreduction of carbon dioxide into formate», *Electrochimica Acta*, vol. 305, mar. 2019, doi: 10.1016/j.electacta.2019.03.066.

[49] W. F. Libby, «Theory of Electron Exchange Reactions in Aqueous Solution», *J. Phys. Chem.*, vol. 56, fasc. 7, pp. 863–868, lug. 1952, doi: 10.1021/j150499a010.

[50] J. E. B. Randles, «Kinetics of rapid electrode reactions», *Discuss. Faraday Soc.*, vol. 1, p. 11, 1947, doi: 10.1039/df9470100011.

[51] J. B. Coon, R. E. DeWames, e C. M. Loyd, «The Franck-Condon principle and the structures of excited electronic states of molecules», *J. Mol. Spectrosc.*, vol. 8, fasc. 1, pp. 285–299, gen. 1962, doi: 10.1016/0022-2852(62)90029-2.

[52] S. Ašperger, «Electron-Transfer Reactions», in *Chemical Kinetics and Inorganic Reaction Mechanisms*, S. Ašperger, A c. di, Boston, MA: Springer US, 2003, pp. 177–201. doi: 10.1007/978-1-4419-9276-5_6.

[53] J. Weiss e E. K. Rideal, «On the theory of electron-transfer processes in aqueous solutions», *Proc. R. Soc. Lond. Ser. Math. Phys. Sci.*, vol. 222, fasc. 1148, pp. 128–141, gen. 1997, doi: 10.1098/rspa.1954.0058.

[54] N. S. Hush, «Adiabatic theory of outer sphere electron-transfer reactions in solution», *Trans. Faraday Soc.*, vol. 57, p. 557, 1961, doi: 10.1039/tf9615700557.

[55] R. A. Marcus, «Chemical and Electrochemical Electron-Transfer Theory», *Annu. Rev. Phys. Chem.*, vol. 15, fasc. 1, pp. 155–196, 1964, doi: 10.1146/annurev.pc.15.100164.001103.

[56] R. A. Marcus e N. Sutin, «Application of electron-transfer theory to several systems of biological interest», *Workshop on antennas and reaction centers of photosynthetic bacteria - structure, interactions and dynamics, Feldafing, F.R. Germany, 23 Mar 1985*, 1 gennaio 1985. https://digital.library.unt.edu/ark:/67531/metadc1070679/m1/6/.

[57] J. R. Bolton e M. D. Archer, «Basic Electron-Transfer Theory», in *Electron Transfer in Inorganic, Organic, and Biological Systems*, in Advances in Chemistry, no. 228, vol. 228. American Chemical Society, 1991, pp. 7–23. doi: 10.1021/ba-1991-0228.ch002.

[58] «Nuclear, electronic, and frequency factors in electron transfer reactions | Accounts of Chemical Research». https://pubs-acs-org.ezproxy.biblio.polito.it/doi/abs/10.1021/ar00081a002.

[59] E. Laviron, «General expression of the linear potential sweep voltammogram in the case of diffusionless electrochemical systems», *J. Electroanal. Chem. Interfacial Electrochem.*, vol. 101, fasc. 1, pp. 19–28, lug. 1979, doi: 10.1016/S0022-0728(79)80075-3.

[60] J. H. Adair, E. Suvaci, e J. Sindel, «Surface and Colloid Chemistry», in *Encyclopedia of Materials: Science and Technology*, K. H. J. Buschow, R. W. Cahn, M. C. Flemings, B. Ilschner, E. J. Kramer, S. Mahajan, e P. Veyssière, A c. di, Oxford: Elsevier, 2001, pp. 1–10. doi: 10.1016/B0-08-043152-6/01622-3.

[61] J. B. Adams, «Bonding Energy Models», in *Encyclopedia of Materials: Science and Technology*, K. H. J. Buschow, R. W. Cahn, M. C. Flemings, B. Ilschner, E. J. Kramer, S. Mahajan, e P. Veyssière, A c. di, Oxford: Elsevier, 2001, pp. 763–767. doi: 10.1016/B0-08-043152-6/00146-7.

[62] object Object, «Correlation between colloidal stability and surfactant adsorption/association phenomena studied by light scattering», Consultato: 4 settembre 2023. [Online]. Disponibile su: https://core.ac.uk/reader/220685500

[63] G. Liu *et al.*, «Research on nonenzymatic electrochemical sensor using HO-BiONO3 nanocomposites for glucose detection», *Sens. Actuators B Chem.*, vol. 242, pp. 484–491, apr. 2017, doi: 10.1016/j.snb.2016.11.019.

[64] S. R. Williams, D. A. Nix, e K. H. Patel, «Drug Storage and Stability», Elsevier, 2007, pp. 2251–2260. doi: 10.1016/B978-0-323-03228-5.50103-8.

[65] N. S. Ghanayem *et al.*, «Stability of dopamine and epinephrine solutions up to 84 hours», *Pediatr. Crit. Care Med.*, vol. 2, fasc. 4, p. 315, ott. 2001.

[66] K. B. Mabrouk, T. H. Kauffmann, e M. D. Fontana, «Abilities of Raman sensor to probe pollutants in water», *J. Phys. Conf. Ser.*, vol. 450, fasc. 1, p. 012014, giu. 2013, doi: 10.1088/1742-6596/450/1/012014.

[67] M. Jackson *et al.*, «An overview of selected current approaches to the characterization of aqueous inorganic clusters», *Dalton Trans. Camb. Engl. 2003*, vol. 44, lug. 2015, doi: 10.1039/c5dt01268f.

[68] L. A. Giannuzzi, «Scanning Electron Microscopy and X-Ray Microanalysis 4th Edition, Joseph I. Goldstein, Dale E. Newbury, Joseph R. Michael, Nicholas W.M. Ritchie, John Henry J. Scott, David C. Joy, Springer, 2018, 550 pp. ISBN:978-1-4939-6674-5.», *Microsc. Microanal.*, vol. 24, fasc. 6, pp. 768–768, dic. 2018, doi: 10.1017/S1431927618015271.

[69] A. Ch. Lazanas e M. I. Prodromidis, «Electrochemical Impedance Spectroscopy─A Tutorial», *ACS Meas. Sci. Au*, vol. 3, fasc. 3, pp. 162–193, giu. 2023, doi: 10.1021/acsmeasuresciau.2c00070.

[70] G. Filho *et al.*, «Controlled release of drugs from cellulose acetate matrices produced from sugarcane bagasse: Monitoring by square-wave voltammetry», *Drug Dev. Ind. Pharm.*, vol. 42, pp. 1–7, nov. 2015, doi: 10.3109/03639045.2015.1107093.

[71] J. Breczko, M. Plonska-Brzezinska, e L. Echegoyen, «Electrochemical oxidation and determination of dopamine in the presence of uric and ascorbic acids using CNOs/PDDA composite», *Electrochimica Acta*, vol. 72, pp. 61–67, gen. 2012.

[72] B. J. Venton e Q. Cao, «Fundamentals of Fast-Scan Cyclic Voltammetry for Dopamine Detection», *The Analyst*, vol. 145, fasc. 4, pp. 1158–1168, feb. 2020, doi: 10.1039/c9an01586h.

[73] L. Chelmea *et al.*, «New Trends in Uric Acid Electroanalysis», *Chemosensors*, vol. 11, fasc. 6, Art. fasc. 6, giu. 2023, doi: 10.3390/chemosensors11060341.

[74] C. Crosnier de Lassichere, L. Latapie, D. Evrard, e P. Gros, «New Insight into the EC' Mechanism of Uric Acid Regeneration in the Presence of Ascorbic Acid on a Poly(3,4-ethylenedioxithiophene) Modified Gold Electrode», *Electroanalysis*, vol. 30, fasc. 8, pp. 1653–1658, ago. 2018, doi: 10.1002/elan.201800024.